Measurements for anomaly detection: the case of diagnostics for disruption prediction in Tokamaks

Authors: A.Murari, T.Craciunescu, M.Gelfusa, E.Peluso, G Rattà, R.Rossi, and J.Vega

Many Thanks to PMU, JEU, TF leaders, Project leaders, Operator, Secondees, Associations and International Partners

CONSORZIO RFX
Ricerca Formazione Innovazione
Institute for Atomic Physics ROMANIA
Ciemat
Università degli Studi di Roma Tor Vergata
Quantum Electronic and Plasma Physics research group
Department of Industrial Engineering

This work has been carried out within the framework of the EUROfusion Consortium and has received funding from the European Union's Horizon 2020 research and innovation programme under grant agreement number 633053. The views and opinions expressed herein do not necessarily reflect those of the European Commission.

Investigation of Collapse

Many natural and man-made systems are stable for long times and look quite resilient but are nonetheless prone to catastrophic collapse.

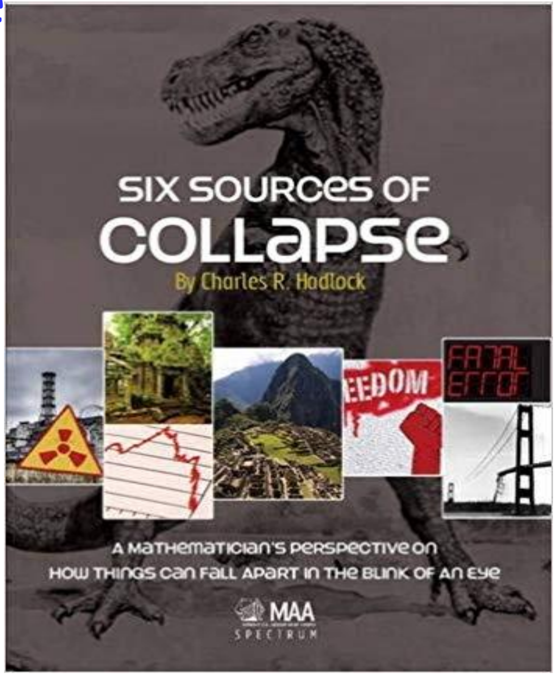

Some of these collapses are quite straightforward to interpret and do not seem worthy of particular attention because, given the proper precautions, they are relatively easy to avoid. Others are very subtle and extremely difficult to predict. Earthquakes, and in general failures due to atmospheric phenomena, belong to the second category.

Disruptions in Tokamaks also fall in the category of catastrophic phenomena very difficult to predict.

Disruption caught on camera on JET

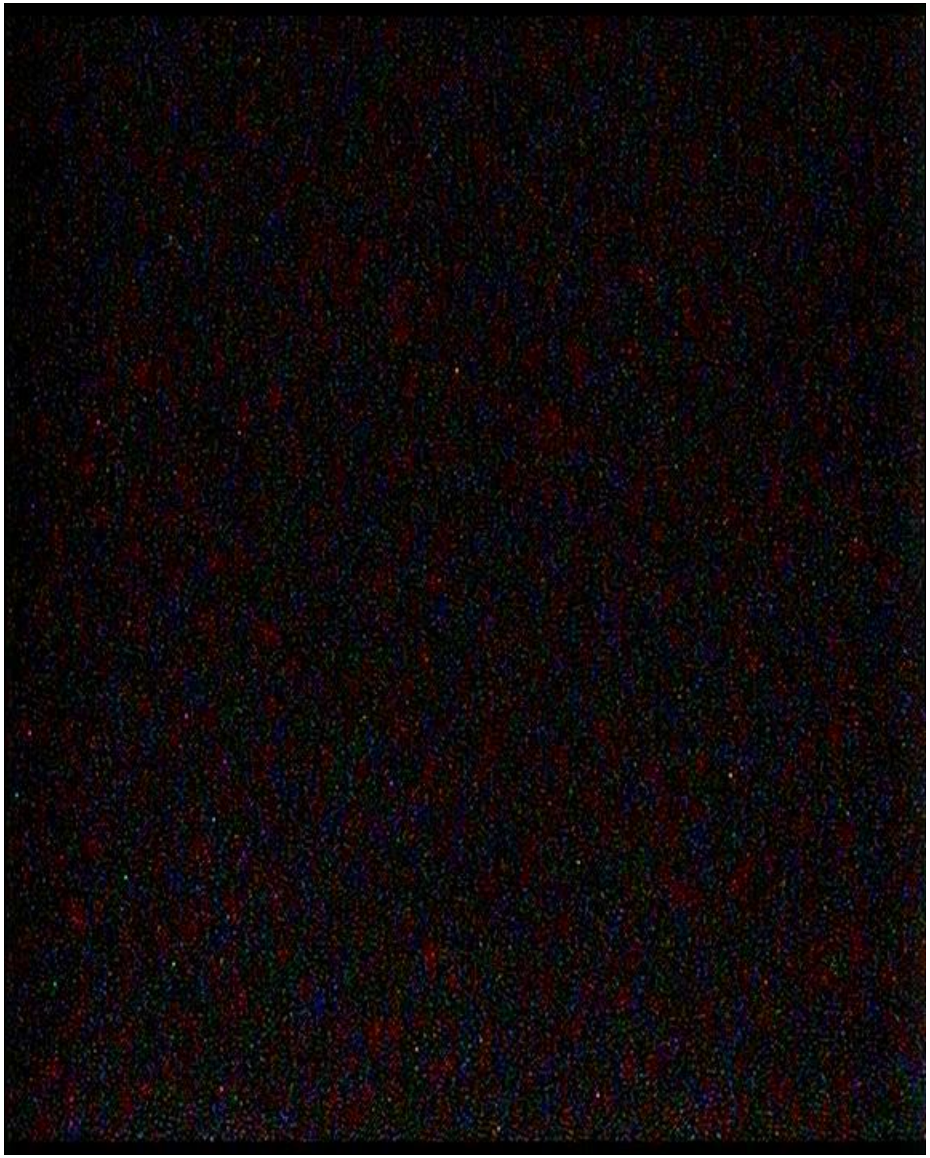

Disruptions in Tokamaks have proved to be unavoidable so far.

Expecting that Tokamak plasmas will never disrupt is like saying that planes will not fall from the sky any more

- Disruptions are sudden losses of confinement and control, which lead to the fast extinction of the plasma current.

- The fast quench phase is normally called thermal quench (loss of kinetic energy) and the slow quench is called the current quench.

- In JET with the ILW the current quench has become much longer (hundreds of ms instead of tens) compared to the carbon wall

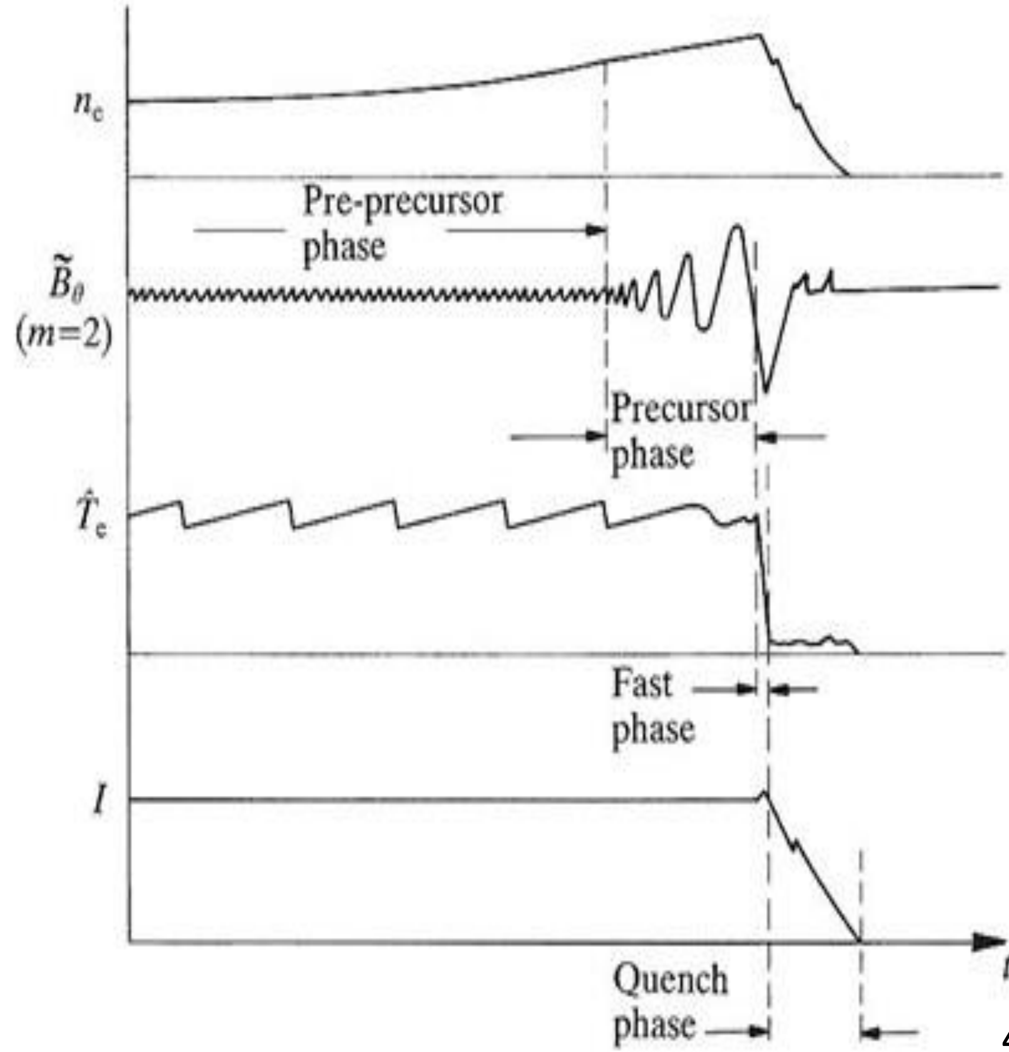

Disruptions and their consequences

The main issues related to disruptions, in addition to lost time, are:

- thermal loads on the plasma facing components,
- forces on the electromagnetic structures,
- runaway electrons.

- The damage to the devices can be severe and the problem scales badly with dimensions. In DEMO even a single, full current, fully mitigated disruption can cause irreparable damage to the device.

Protection ITER wall against disruptions

ITER divertor melt avoidance requires high radiated fractions

- Critical heat flux factor for tungsten is $50\ MJ/m^2 s^{0.5}$
- Divertor thermal quench (TQ) heat flux area of 23 m^2 *, and thermal quench duration of $\tau_{tq} \approx 1$ ms

$$\frac{350\ MJ}{23\ m^2\sqrt{10^{-3}\ s}} = 480\ MJ/m^2 s^{0.5}$$

- Conducted heat loads must be less than 10% and the thermal radiated fraction $f_{rad,th}$ **must exceed 0.9**

ITER first wall melt avoidance requires low radiation peaking factors

- The melt temperature of Be is $T_{lim} = 1551$ K, and the first wall can reach $T_{0,fw} = 600$ K
- Maximum allowable **peaking factor is about 2**

*V. Riccardo et al., Nucl. Fusion **45** (2005)
** M. Lehnen et al., J. Nucl. Mater. **463** (2015)

Classification of diagnostics for disruptions

The disruption diagnostics are essential for all the PEC objectives of science (prediction, explanation and control).

A possible classification of diagnostics is:

- Diagnostics for monitoring the consequences.
- Diagnostics for the disruptions themselves (runaway electrons).
- Diagnostics for the investigation of the physics.
- Diagnostics for prediction.

- Understanding the physics is essential for the extrapolation to next devices
- Prediction is essential for triggering any remedial action.

Diagnosing for disruptions: control

- Diagnostics for disruptions must be seen in context of the control systems and the actuators.

- Hardware: the emphasis is therefore on reliability, availability, time and spatial resolution, coverage etc.

- The first signal processing requires specific techniques to provide adequate inputs to the predictors and control systems.

- Predictive capability: they have to be combined with effective and reliable prediction tools deployable in real time.

Outline

- Disruptions in the context of control and countermeasures
- Requirements of diagnostics with particular attention to physics and prediction
    - Hardware: Coils, cameras and bolometry
    - Profile indicators
    - Tomography
- Data analysis tools for prediction
- Conclusions and future work

Disruptivity in metallic devices

JET: baseline high current q_{95} around 3 (reference scenario for ITER) in preparation for DT in some campaigns were affected by disruptivity of the order of 60%. Also the hybrid at high current does not meet the requirements of ITER

WEST: disruptivity never below 70% in all campaigns so far

The reactor will have to work at more than 90% radiation fraction, detached divertor, above Greenwald limit, all conditions increasing disruptivity.

- A typical disruption pattern for metallic wall tokamaks is the core accumulation of heavy impurities which affect **core power balance by radiating** and generate MHD unstable current profiles

P.C. de Vries, Nucl. Fus. 2012

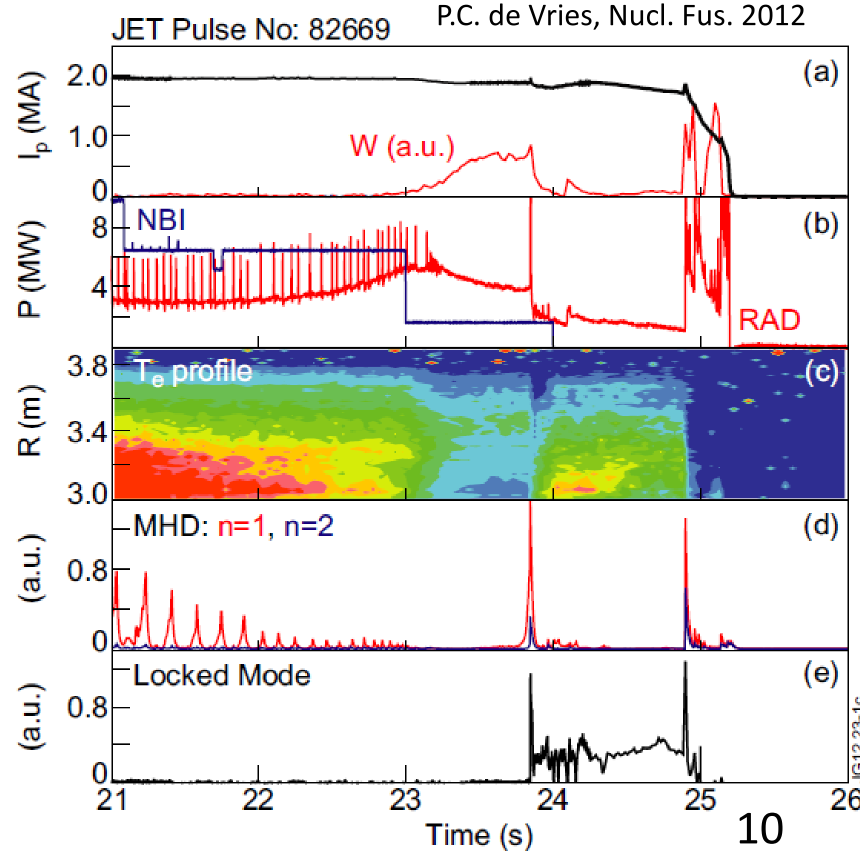

- Definition of the discharge phases with respect to disruptions

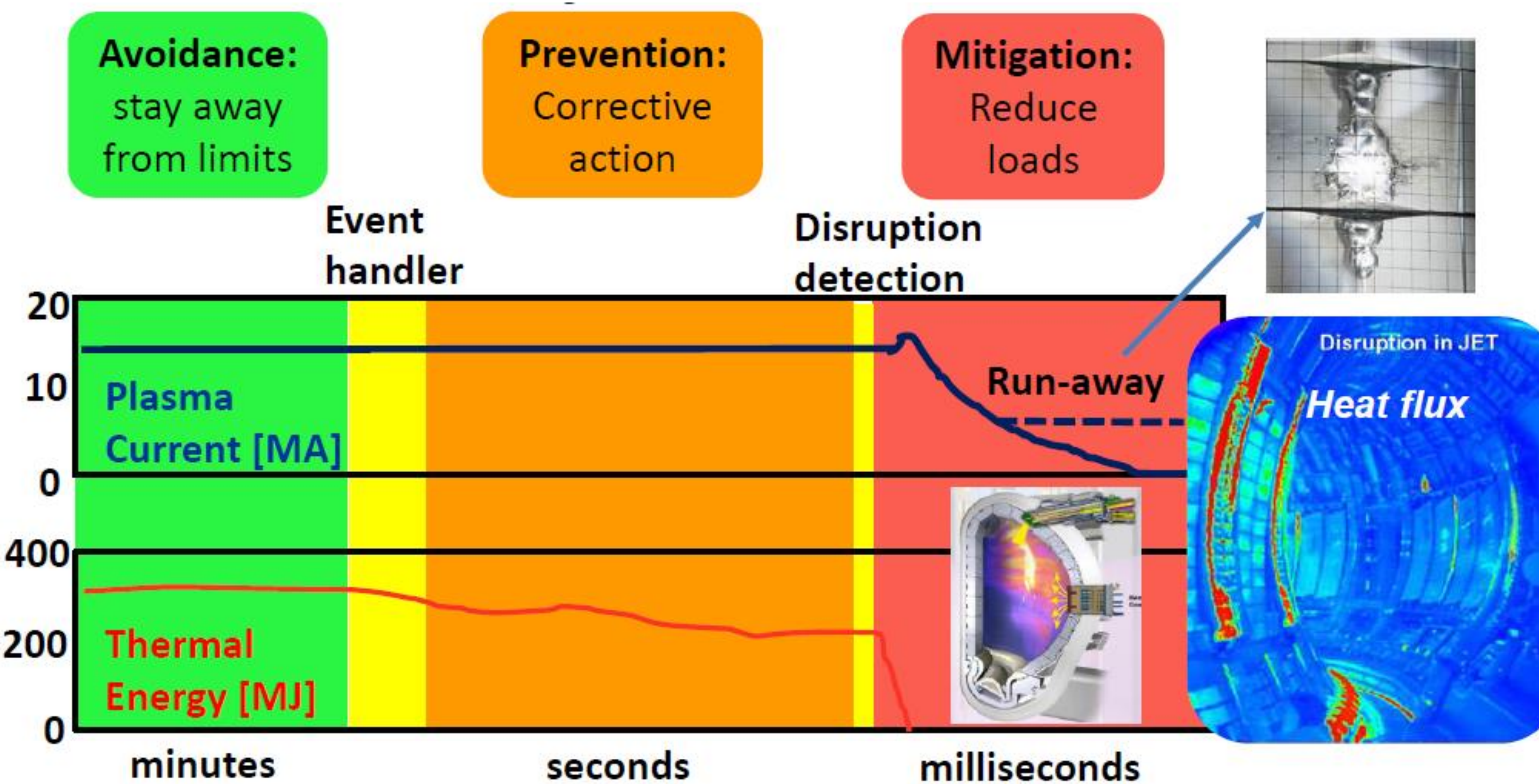

Outline

- Disruptions in the context of control and countermeasures
- Requirements of diagnostics with particular attention to physics and prediction
    - Hardware: Coils, cameras and bolometry
    - Profile indicators
    - Tomography
- Data analysis tools for prediction
- Conclusions and future work

Locked mode detection on AUG

The growing and locking of MHD modes are among the main causes of disruptions in TOKAMAKS.

Typically, m/n= [1/1 ; 2/1] islands are observed both at AUG and JET and are also coupled with m/n=3/1 modes. The growth rate and the width of such instabilities depend on the **radial component** $\boldsymbol{B_1^r}$ of the magnetic field and, consequently, its measurement is an important element to prevent disruptions.

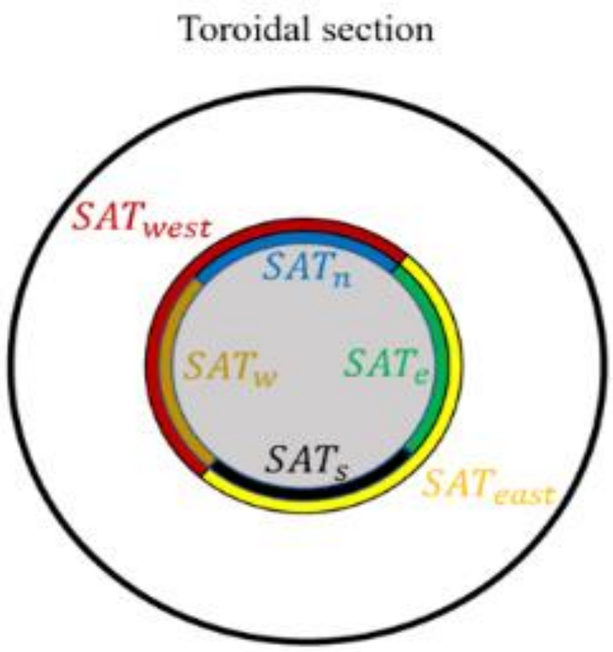

A lot of efforts are being exerted to counteract locking of mode to the wall, from ECE feedback control of NTMs to rotating perturbations.

AUG: top of the actual arrangements of the two saddle coil systems one composed by two saddle coils (SATwest and SATeast) and another one composed by four coils (Satn, Sats, Sate, Satw).

New indicator $f(t)$ for slowing down

A frequency indicator based on the weighted mean of the FFT spectra of both radial perturbations has been tested:

$$f_{ew} = \frac{\sum f_i I_{ew}(t, f_i)}{\sum I_{ew}(t, f_i)} \qquad f_{ns} = \frac{\sum f_i I_{ns}(t, f_i)}{\sum I_{ns}(t, f_i)}$$

f_i is the *i-th* frequency of the FFT spectrum and $I_{ns,ew}(t, f_i)$ is the intensity at the frequency f_i and time *t*. Then, it is possible to average the frequency of rotation as

$$f(t) = \frac{1}{2}[f_{ns}(t) + f_{ew}(t)]$$

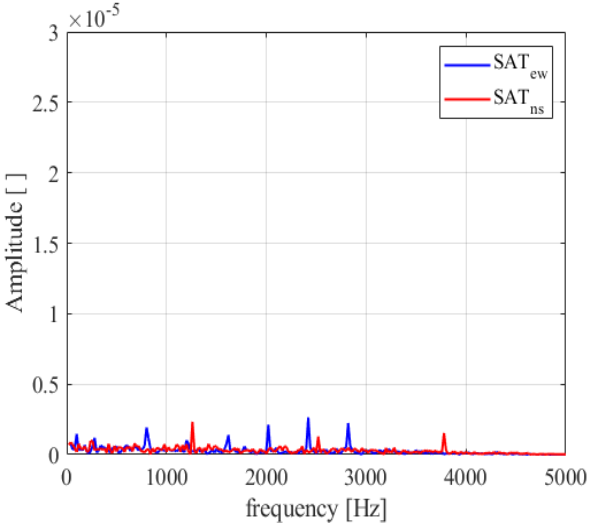

~340ms before the disruption

- pulse 30799;
- disruption at 2.79s;

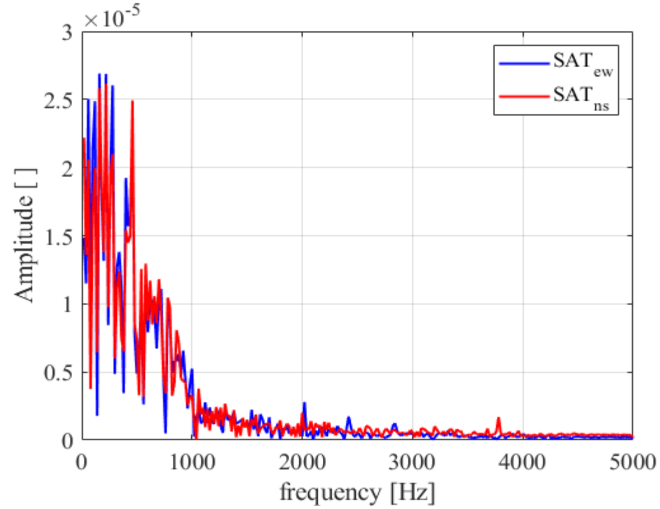

~50ms before the disruption

$f(t)$: minimizing external perturbation

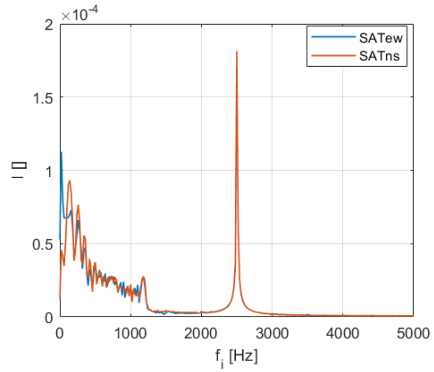

Ms generate a perturbation in the same low frequency range of

Pulse safe with ELMS

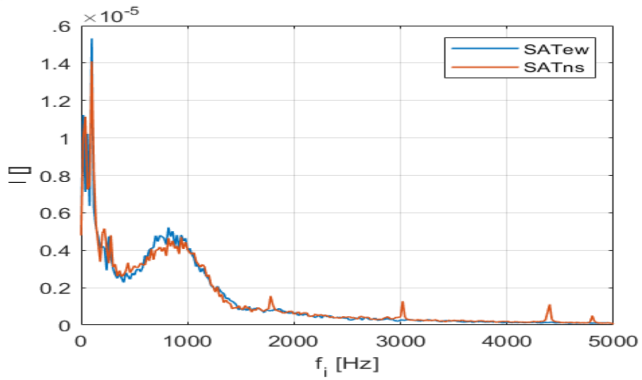

Disruptive pulse

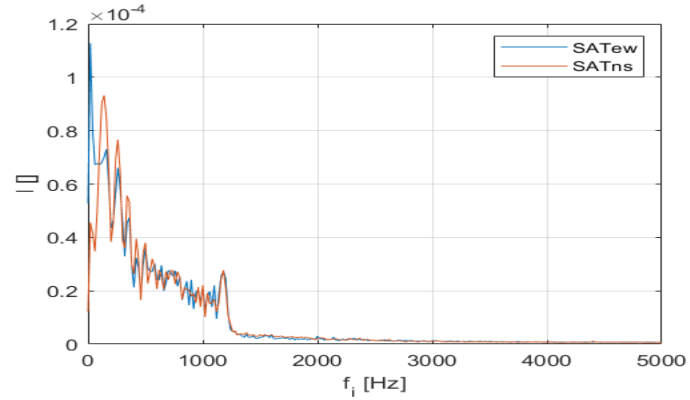

To minimize the effect of external perturbations, namely the influence of ELMs, a driving sinusoidal functions has been added to the radial measurements Bew and Bns.

$$B_r^{ns,adv} = B_r^{ns} + A_0 \sin(\omega_0 t)$$

$$B_r^{ew,adv} = B_r^{ew} + A_0 \sin(\omega_0 t + \psi_0)$$

Pulse safe with ELMS

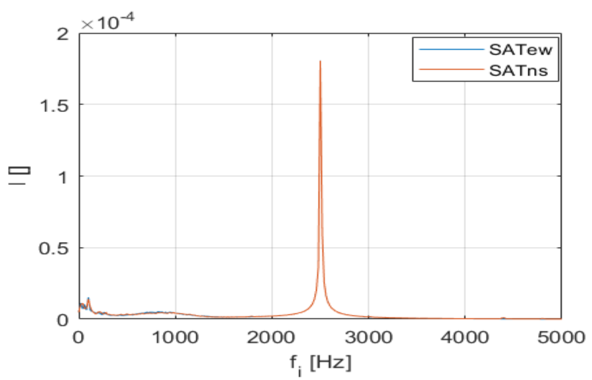

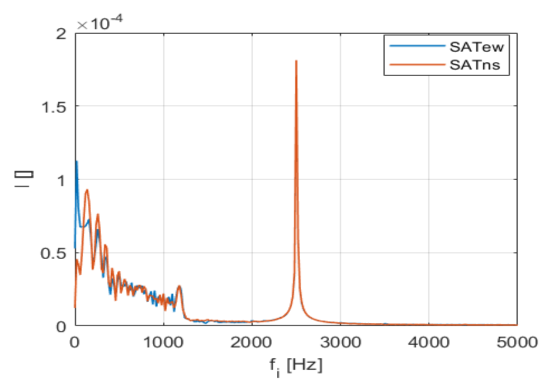

Disruptive Pulse

Imaging of the ITER-like Wall

IR and Vis cameras cover 66% of JET first wall and 47% of JET divertor

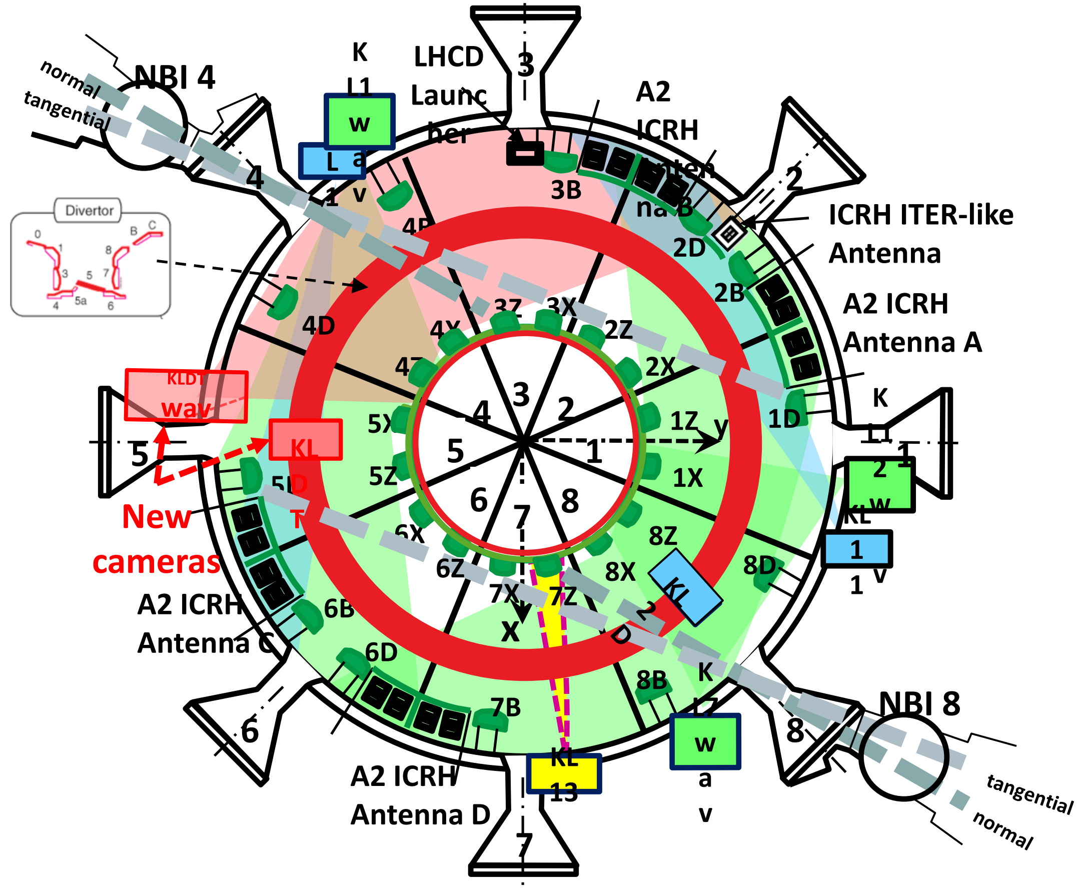

VIS

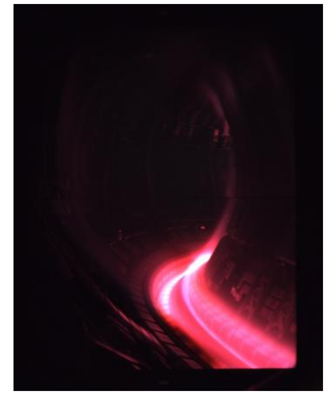

IR

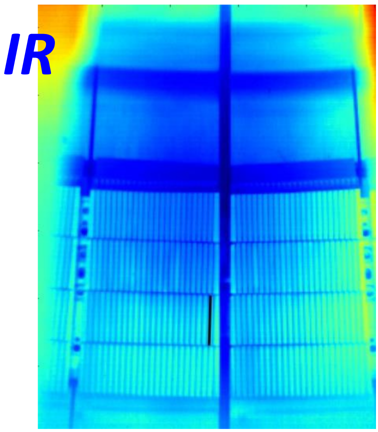

Two views highlighted in red to be made available outside the biological shield: optical path of 42 m for the VIS and 32 for the IR. Important for both machine protection and physics

MARFEs

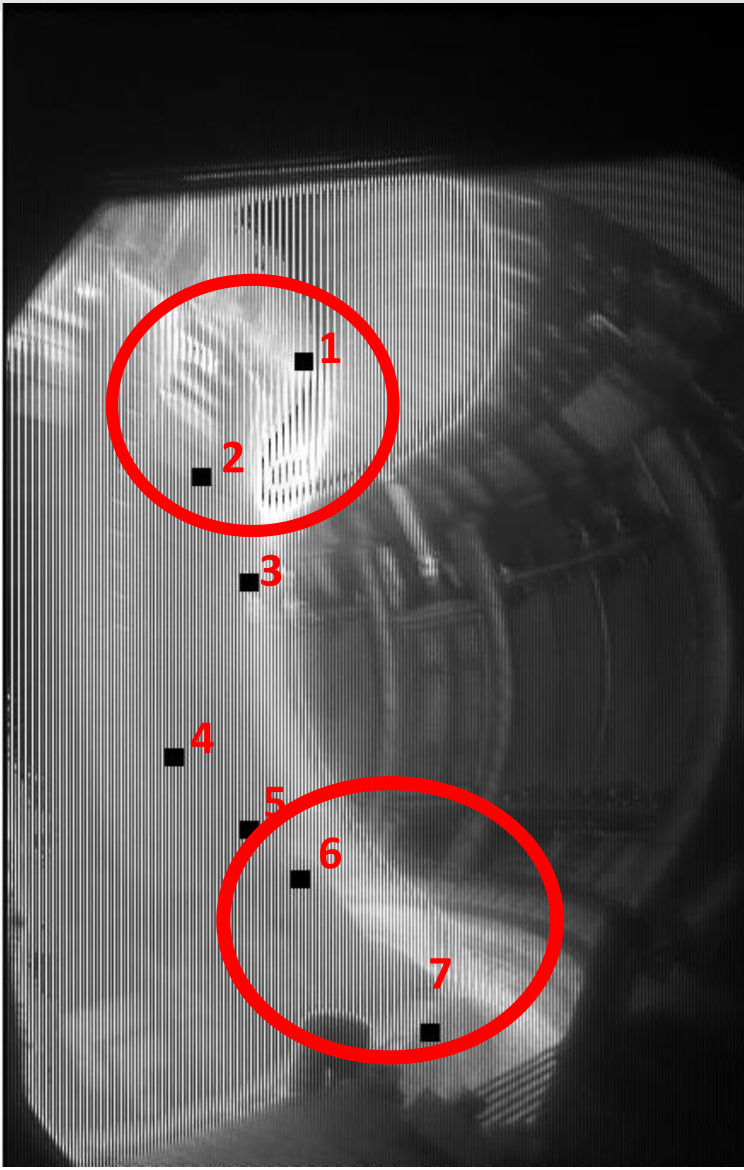

JET #95302.

MARFE are thermal instabilities which manifest themselves as rings of visible radiation.

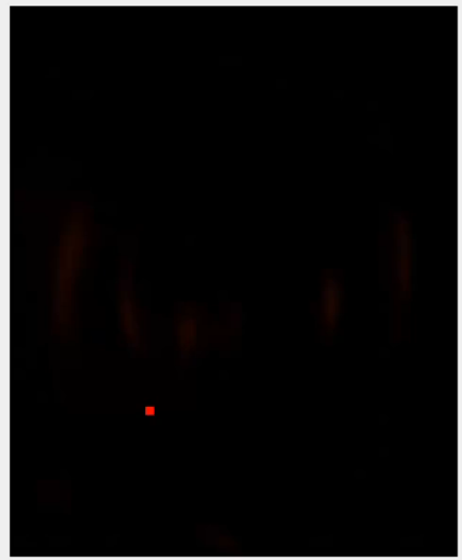

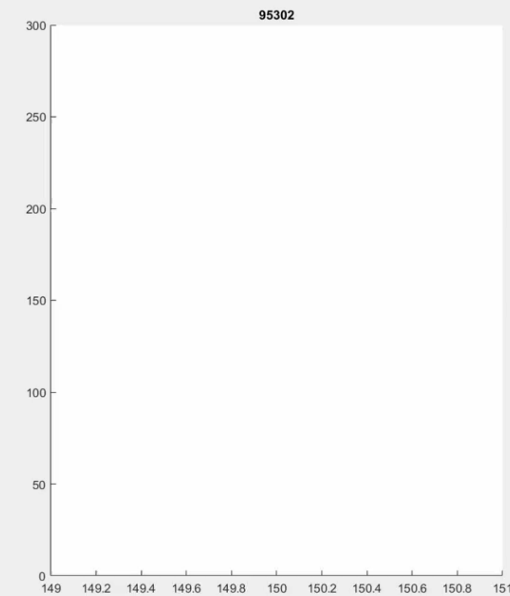

Their signature on the videos can be used for disruption prediction.

Total power loss: bolometry

- Bolometry requires a uniform sensitivity over a large frequency range of ($h\nu$ =1-10000 eV)
- Several detectors have been developed,
- Typically it is a resistance that changes its temperature under irradiation.
- Surface is darkened by graphite deposition or by porous gold.
- Temperature measurements provide the absorbed power

4 det

4 ref

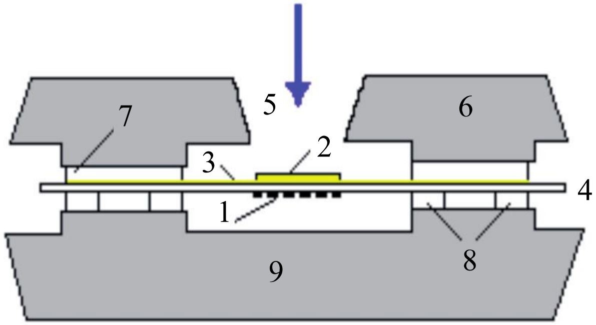

1 Resistor
2 Absorber
3 Foil for thermal contact

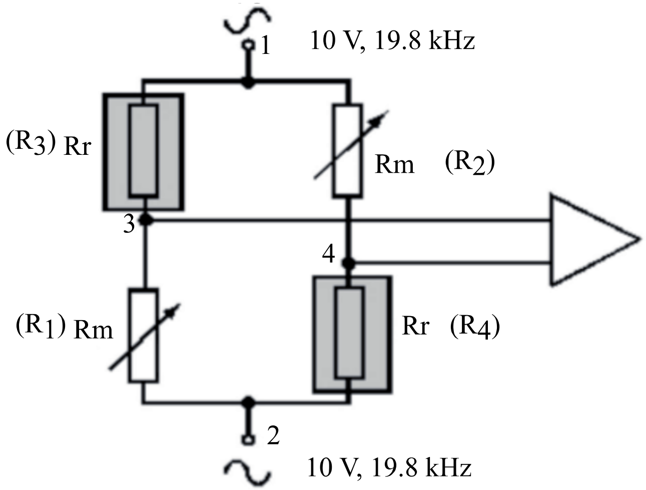

Signal Processing

- Detectors are integrators and require a derivative to obtain the time resolved power.

$$P = C\left(\frac{dV}{dt} + \frac{V}{\tau_c}\right)$$

Problems with metal foil bolometers

- Noise: magnetic compatibility, derivative
- Radiation hardness: gold contacts affected by transmutation
- Calibration: in situ
- Sensitivity to neutrals
- Effects of the ambient gas

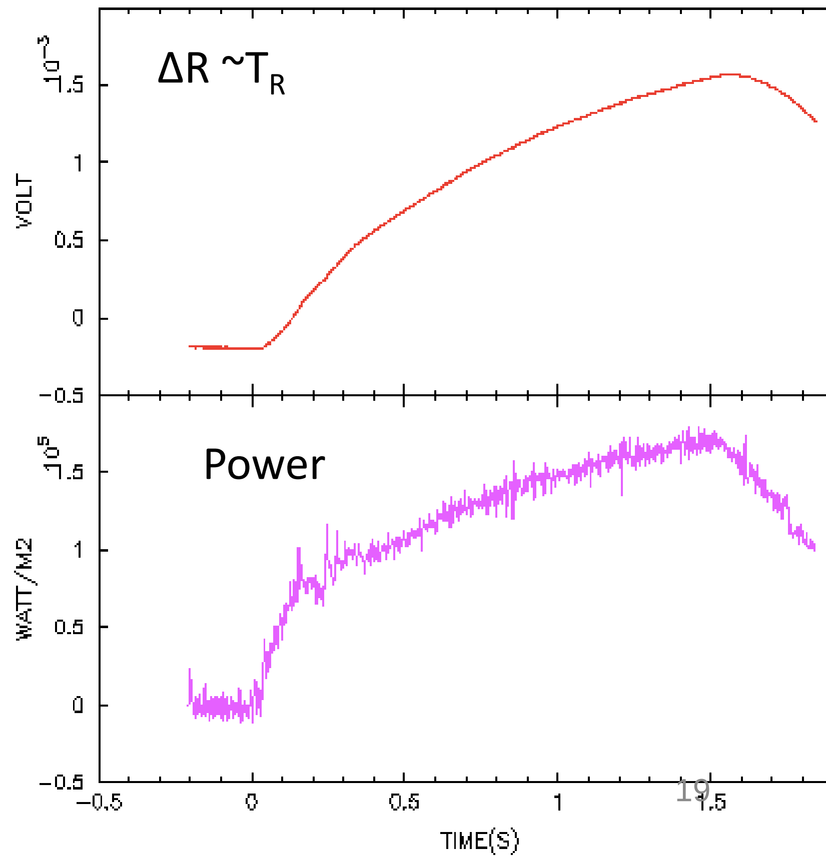

Diamond based bolometers: diodes

- Single crystal diamond Schottky diodes have been proved to reliable devices for plasma diagnostics.
- The radiation hardness of the technology is now well assessed.
- A diamond based bolometric system (5.5 eV – 10 keV energy range) would definitively have higher time resolution (up to 1MHz),

Bandwidth 200 kHz on JET.

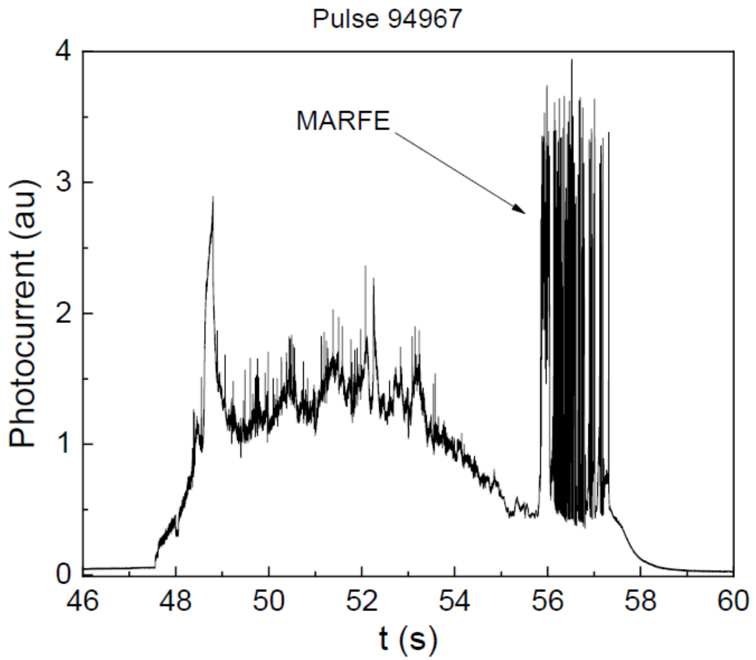

- Such a system would allow to separate the VUV (5.5 eV - 1 keV) and soft-X (1 keV– 10 keV) contributions, for a more detailed analysis of the plasma emission.

Outline

- Disruptions in the context of control and countermeasures
- Requirements of diagnostics with particular attention to physics and prediction
  - Hardware: Coils, cameras and bolometry
  - Profile indicators
  - Tomography
- Data analysis tools for prediction
- Conclusions and future work

Profile measurements

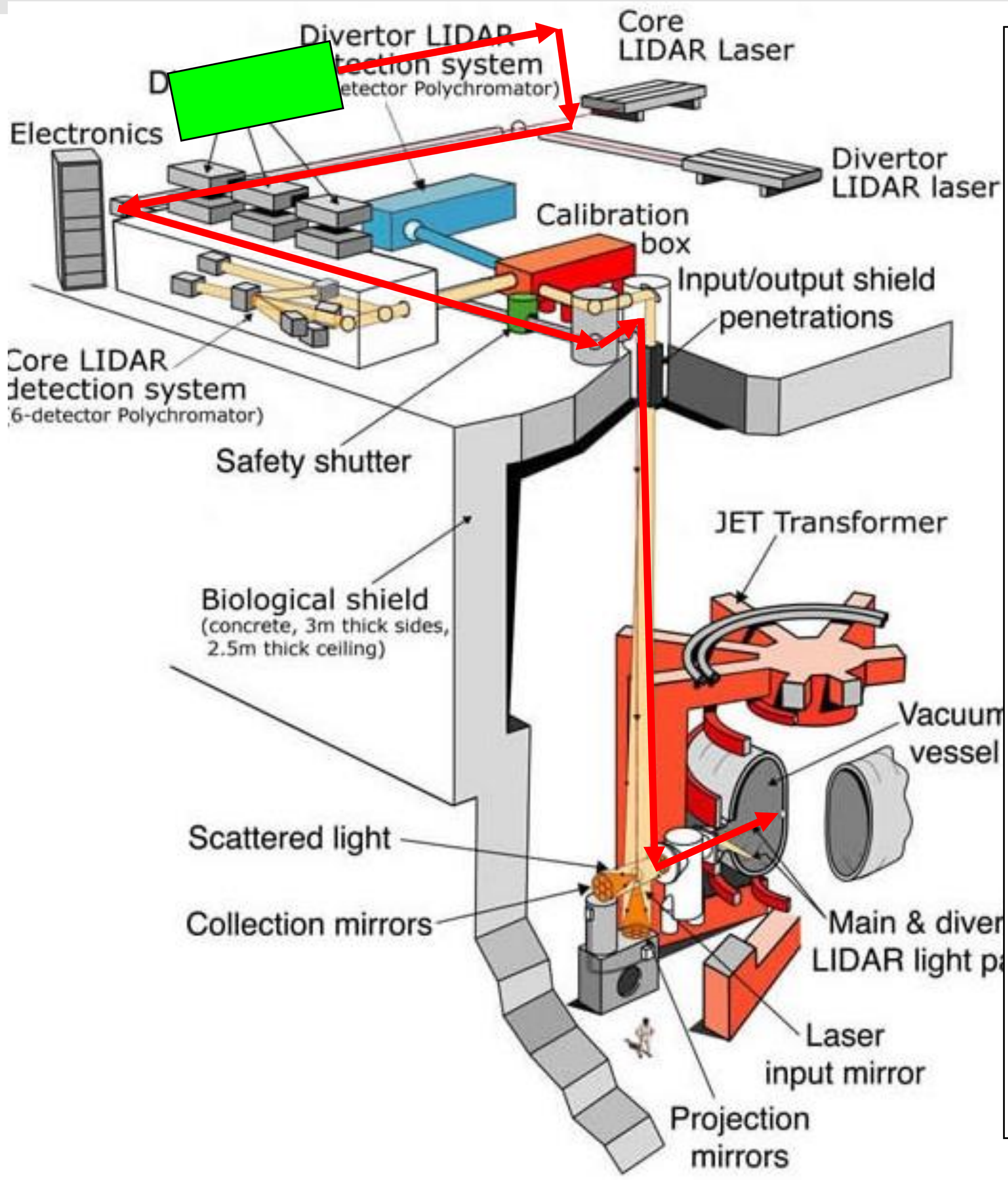

LOCAL MEASUREMENTS

- The percentage of direct, local, spatially resolved measurements is not very high (many are external or integrated see later)
- Some are complementary (ECE, TS), which is extremely important for the physics
- For disruption prediction and feedback control what is often needed are profile indicators.

Profile indicators: hollowness

For disruption prediction profile indicators have to be robust and calculable in real time but at the same time they need to be sufficient informative.

Hollowness is particularly difficult to quantify.

- Mirroring in case of insufficient coverage.
- Resilience against irregularities in the profiles.

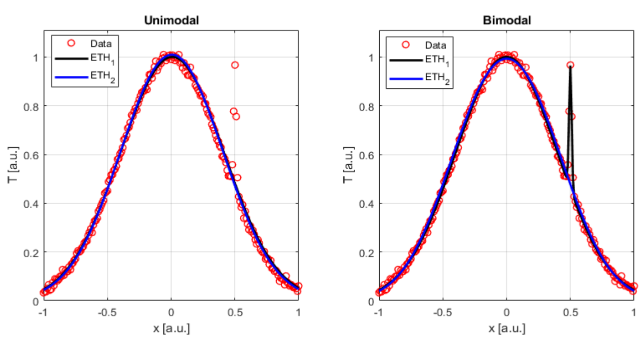

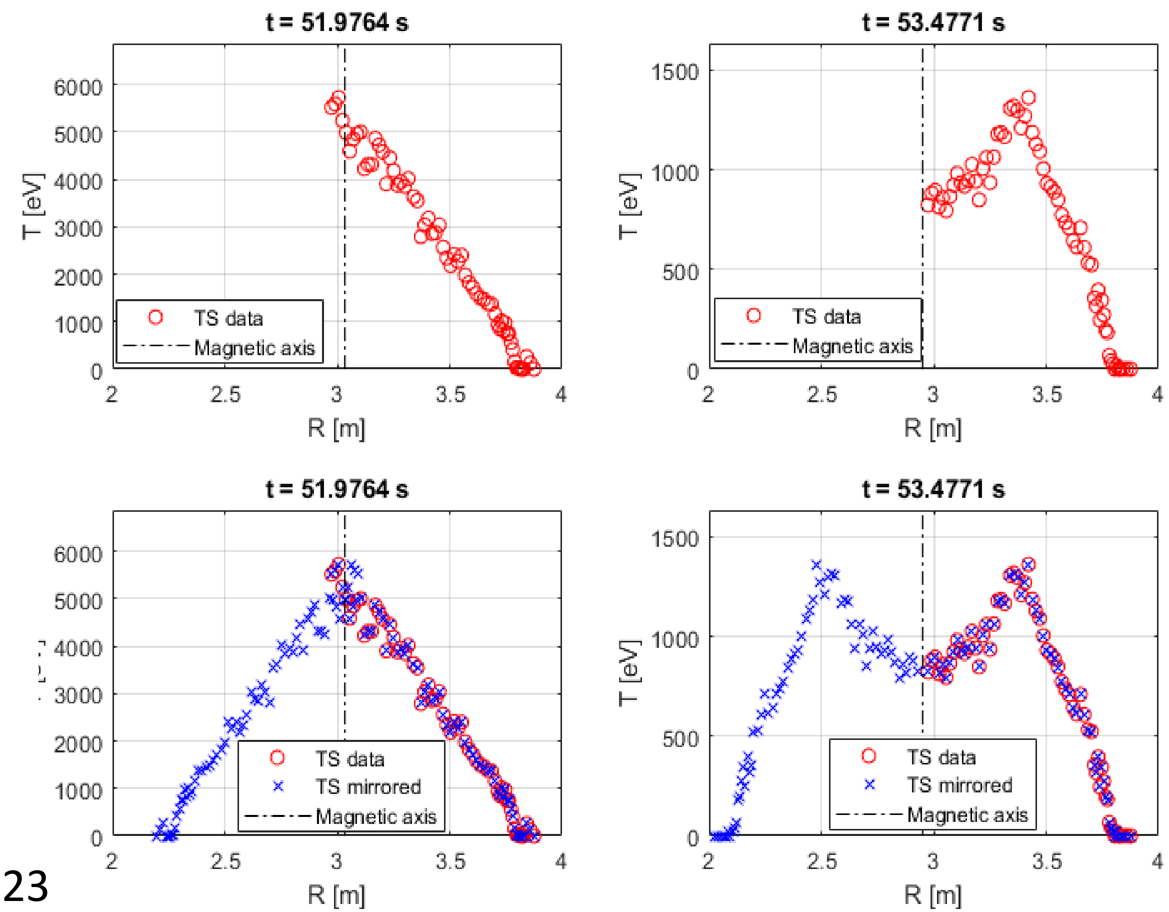

Profile indicators

A good approach is to use some sort of fitting. In our case with two Gaussians for example.

$$y = A_2 e^{-\frac{(x-\mu_2)^2}{2\sigma_2^2}} + A_2 e^{-\frac{(x+\mu_2)^2}{2\sigma_2^2}}$$

Can be solved with the weighted fitting using the Guo method.

$$\begin{bmatrix} \sum y_i^2 & \sum x_i y_i^2 & \sum x_i^2 y_i^2 \\ \sum x_i y_i^2 & \sum x_i^2 y_i^2 & \sum x_i^3 y_i^2 \\ \sum x_i^2 y_i^2 & \sum x_i^3 y_i^2 & \sum x_i^4 y_i^2 \end{bmatrix} \begin{bmatrix} a \\ b \\ c \end{bmatrix} = \begin{bmatrix} \sum y_i^2 \left(\ln(y_i) - \ln\left(1 + e^{-2bx}\right)\right) \\ \sum x_i y_i^2 \left(\ln(y_i) - \ln\left(1 + e^{-2bx}\right)\right) \\ \sum x_i^2 y_i^2 \left(\ln(y_i) - \ln\left(1 + e^{-2bx}\right)\right) \end{bmatrix}$$

An indicator of the Z test type can then be used to quantify the level of hollowness.

$$ETH_{1,B} = \frac{\left|\mu_{2,2} - \mu_{2,1}\right|}{\sqrt{\sigma_{2,1}^2 + \sigma_{2,2}^2}}$$

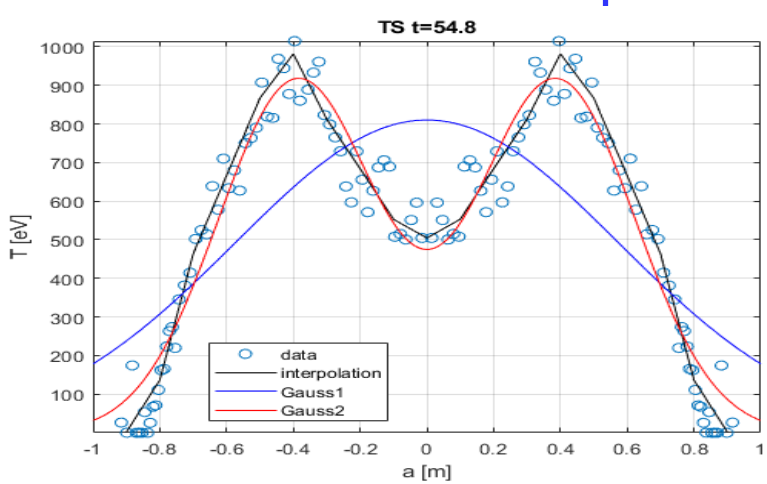

Inverse problems in Fusion

In fusion many measurements require some form of inversion to be interpreted:

- **Magnetic topology** (requires inversion of both external and internal measurements of the field components)
- All the line integrated measurements require some form of inversion (**interferometry**, **tomographies** etc)
- **Camera images** (both visible and infrared)
- **Several detectors** require unfolding (inversion in energy space)

Unfortunately many inverse problems are ill-posed

Ill-posed problems

If **D** is the space of the data or measurements, **S** the source and **A** the forward function mapping the reality on the space of the measurements

$$D = A(S)$$

The task of recovering **S** from **D** is well posed (accordig to the definition of Hadamard)

- A solution exists for any data **D** in data space
- The solution is unique in the source space **S**
- The inverse mapping **D** → **S** is continuous

- In general the vast majority of inverse problems in fusion are ill posed

→Two main difficulties: how to identify the right solution and how to quantify the uncertainties

→ In tomography solving an ill-posed problem means finding a regularizing algorithm

The tomographic problem

Integrated Data → **Tomographic Inversion** → Local Information

$$g_l = \int f \cdot ds\,, \qquad l = 1, \ldots, n_d$$

f - the local emissivity

g_l - the projection (along the line of sight L)

n_d - number of detectors (or number of projections)

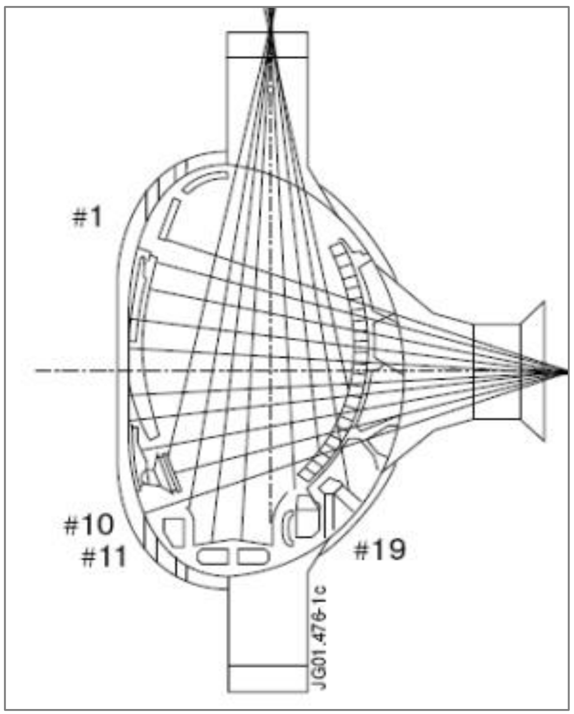

JET γ and neutron

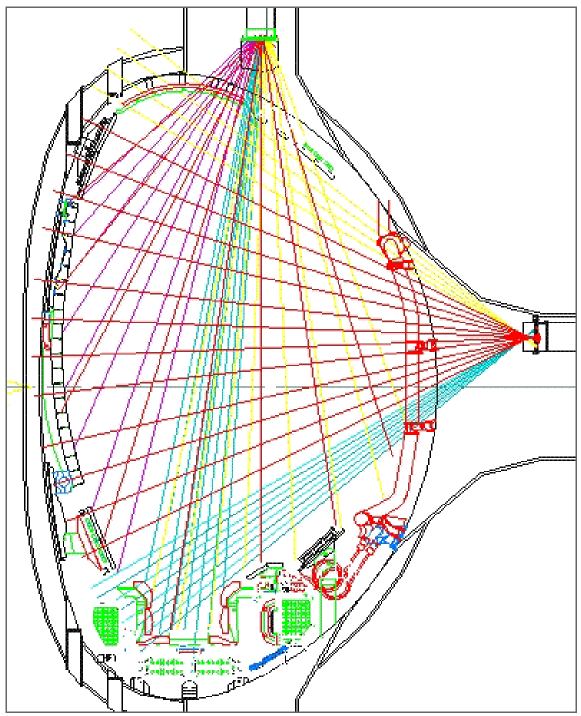

JET bolometer

- Bolometry: two views of 24 chords each.
- Neutron/gamma rays: 10 horizontal channels 9 vertical channels

Maximum Likelihood method (ML)

❖ **Assumption: Emission - a Poisson process**

- g_m **- sample from a Poisson distribution**
- $\bar{g}$ **- expected value**

The probability of obtaining the measurement

$$g = \{g_m | m = 1, \dots, N_d\}$$

if the image is $f = \{f_n | n = 1, \dots, N_p\}$

is given by the likelihood function:

$$L(g/f) = \prod_k \frac{1}{g_k!} (\bar{g})^{g_k} \times exp(\bar{g})$$

❖ **Poisson distribution:**

❖ More accurate for the case of concentrated sources than max entropy which tries to spread as much as possible the solution over the cross section

$$f_{ML} = argmax_f L(g/f)$$

$$f^{(k+1)} = f^k \, diag[\hat{f}^{(k)}] diag[s^{-1}] \left[H^T diag[H\hat{f}^{(k)}]^{-1} g - H^T I\right)\right]$$

f^k can be retrieved by running the ML algorithm with noise-free data

$$\varepsilon^{(k+1)} = $$
$$= diag[\hat{f}^{(k)}] diag[s^{-1}] H^T diag[H\hat{f}^{(k)}]^{-1} n$$
$$+ [I - diag[\hat{f}^{(k)}] diag[s^{-1}] H^T diag[H\hat{f}^{(k)}]^{-1} H] \varepsilon^{(k)}$$

Rule for finding the uncertainty in the current estimate <u>at each iteration</u>

Overview Seeding Experiments

54 discharges at high radiation with N, Ne and Kr have been analyzed.

The experiments analysed in this work were mainly discharges at 2.5MA/2.6T with the strike points on the vertical targets.

The input power ranged between 17 MW and 19 MW, mainly from the neutral beams. A few MW of ICRH were typically injected to avoid impurity accumulation in the core.

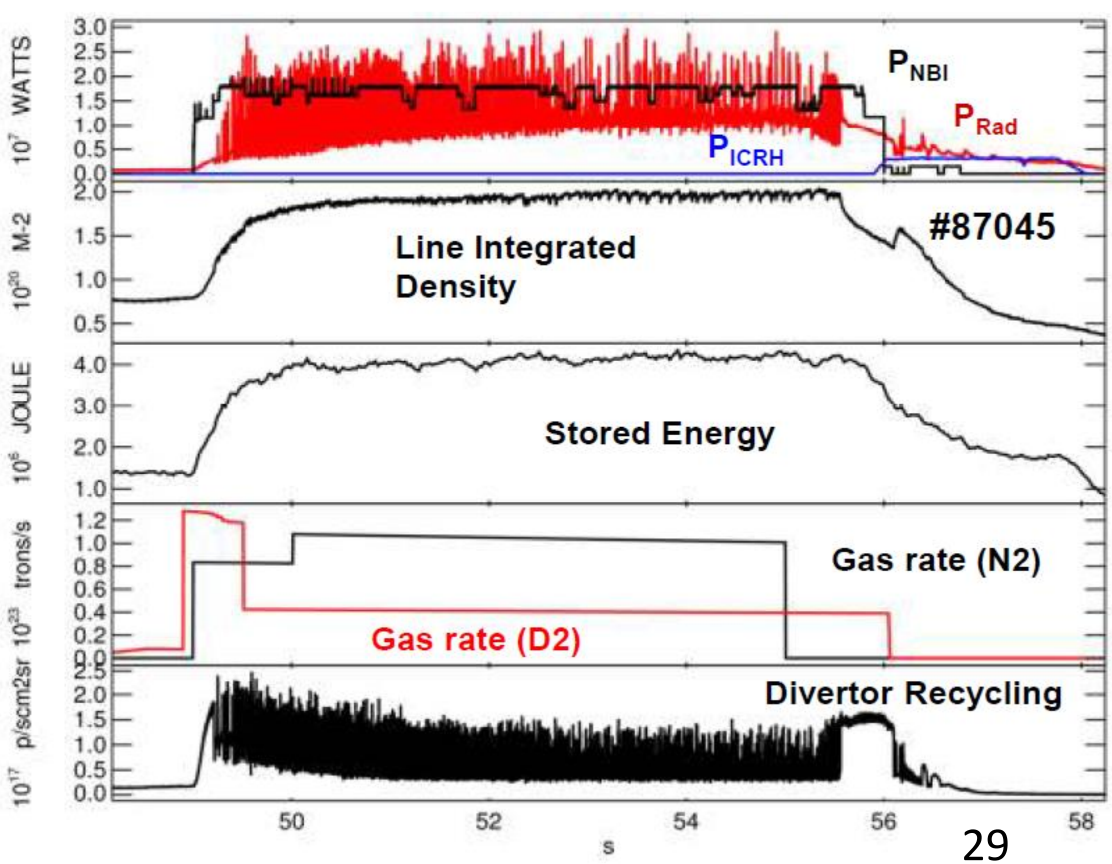

The impurity seeding was performed with valves injecting in the divertor private region. Deuterium fuelled by valves located on the divertor vertical targets.

The bolometric measurements have been properly filtered to eliminate unrealistic values. Signals averaged over 25 ms.

<u>Quantification of the uncertainties is essential</u>

Seeding Experiments: Neon

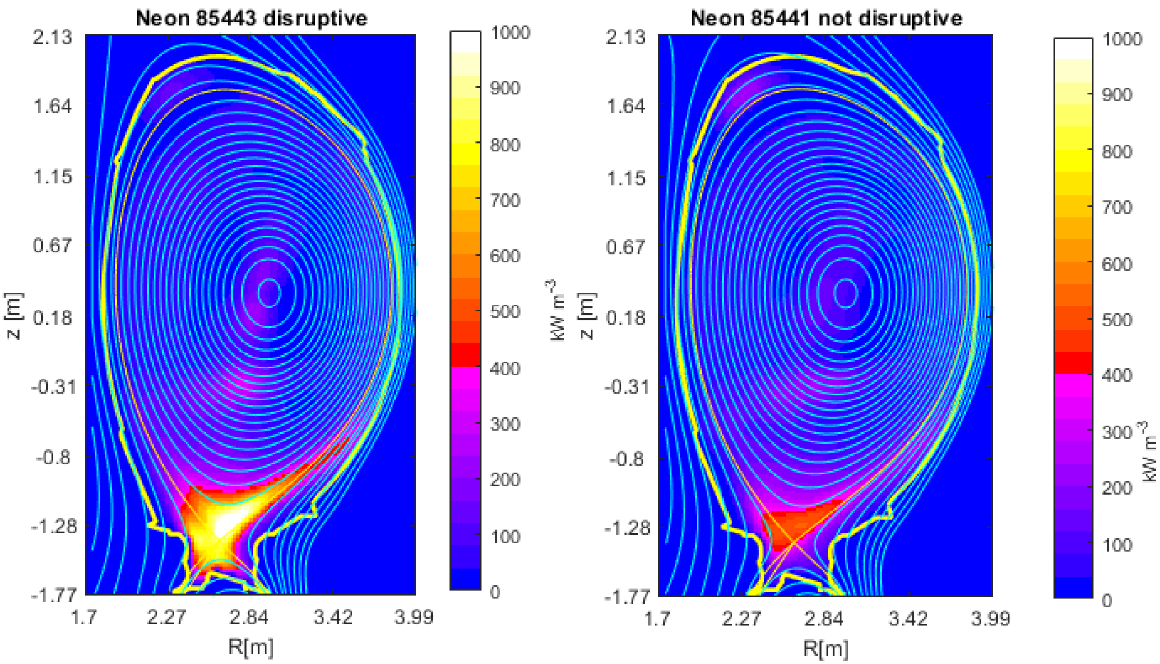

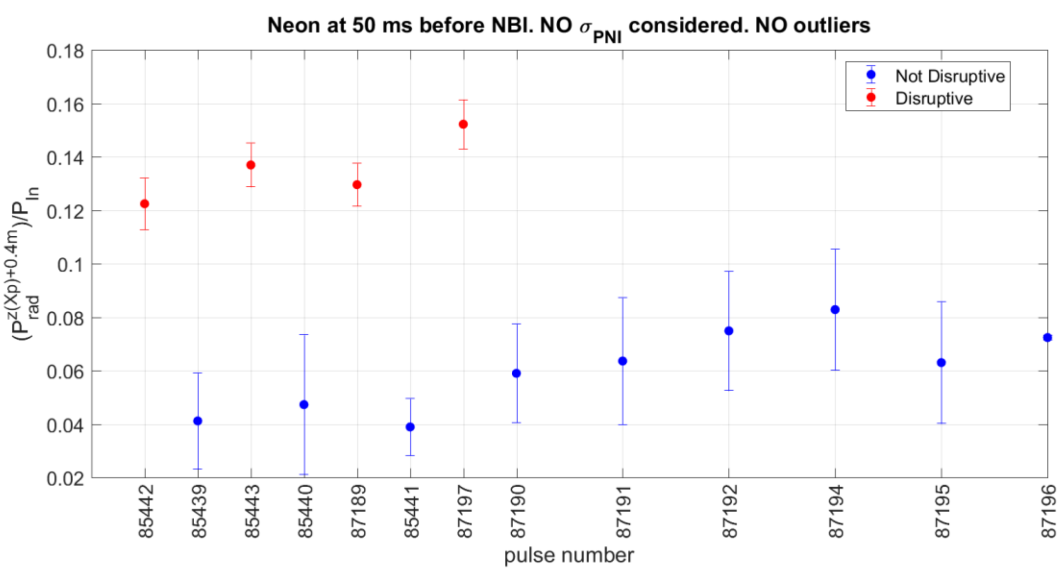

Discharges with N and Neon seeding present a very similar phenomenology.

Max radiated fraction achieved safely is 70% if one believes the estimates of the ML.

The disruption is preceded by the formation of a MARFE type of high radiative zone above the X point.

Shattered Pellet Injector on JET for ITER

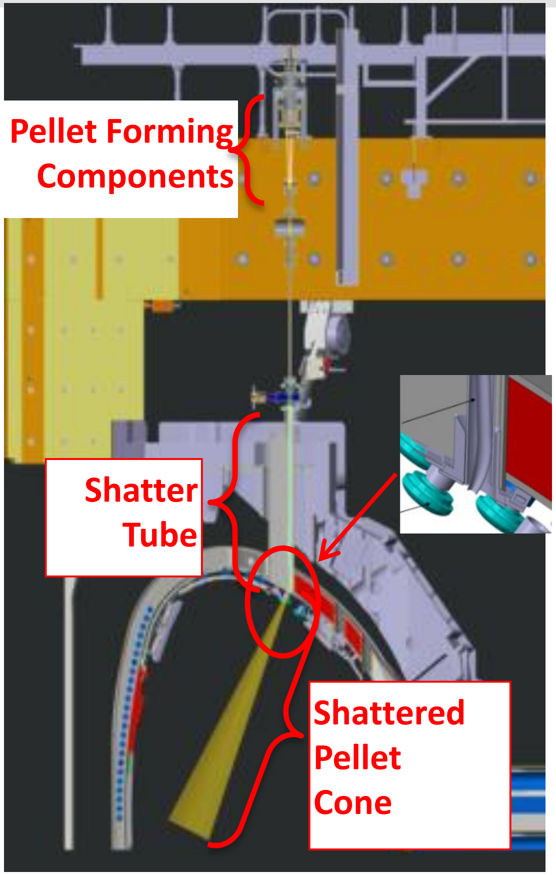

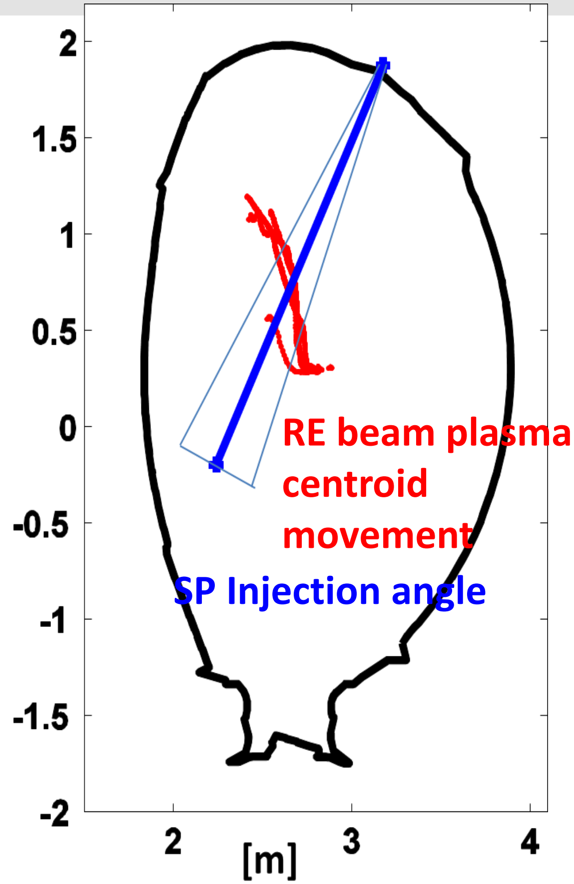

- Trajectory of the run-away beam current centroid measured by the magnetics.
- The beam moves towards the upper –inner board side (where the impacts are also observed)
- The planned cone for the SPI crosses the trajectory of the runaway electron beam

- <u>Runaway electrons</u>: the magnetics based fast control systems can control these beams until they are suppressed with shattered pellets. The optimization requires detailed studies with cameras, bolometry and scintillators .

Detection of runaway electrons

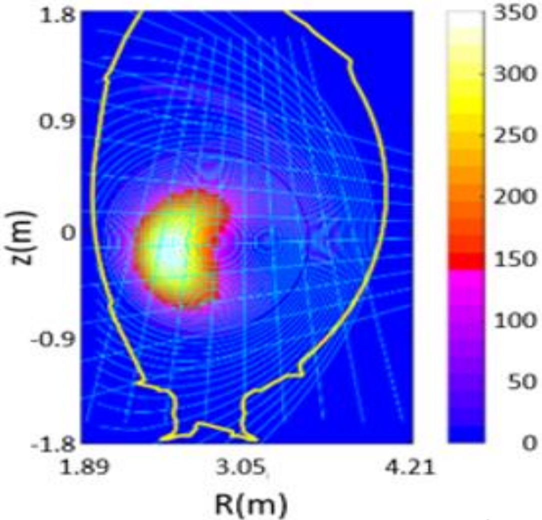

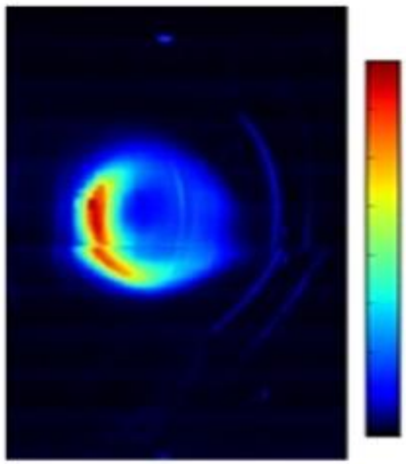

#95128, t=48.41-48.42s

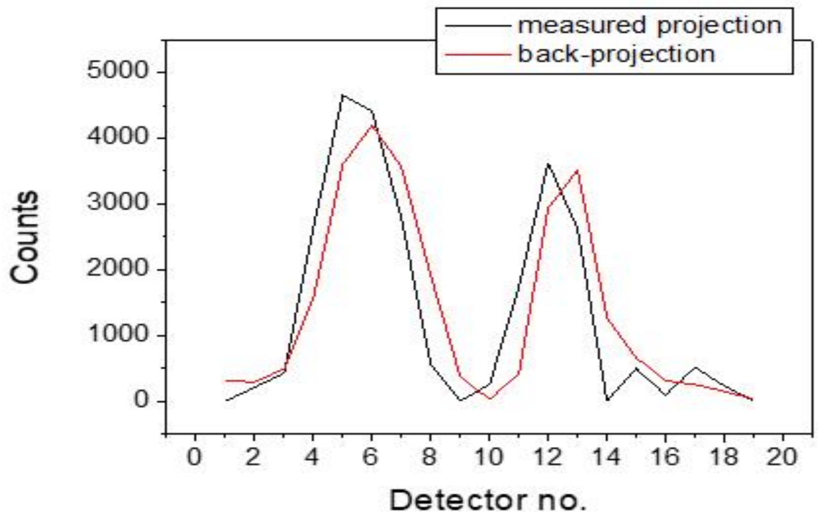

Comparison of

a) Left the tomography of the gamma-ray camera (between 2 and 4 MeV)

b) Right the synchrotron emission with camera

Comparison of line integrals and back projections

Many thanks to Milan Group

M.Gelfusa et al "A Maximum Likelihood Tomographic Method applied to JET Gamma ray Emission during the Current Quench" SOFT 2020

The measurements of the gamma ray cameras have to be integrated (over 10 ms) to improve the photon statistics.

Since the measurements are taken during the current quench, during this interval the plasma can evolve

Magnetic surfaces at the beginning and end of the integration interval

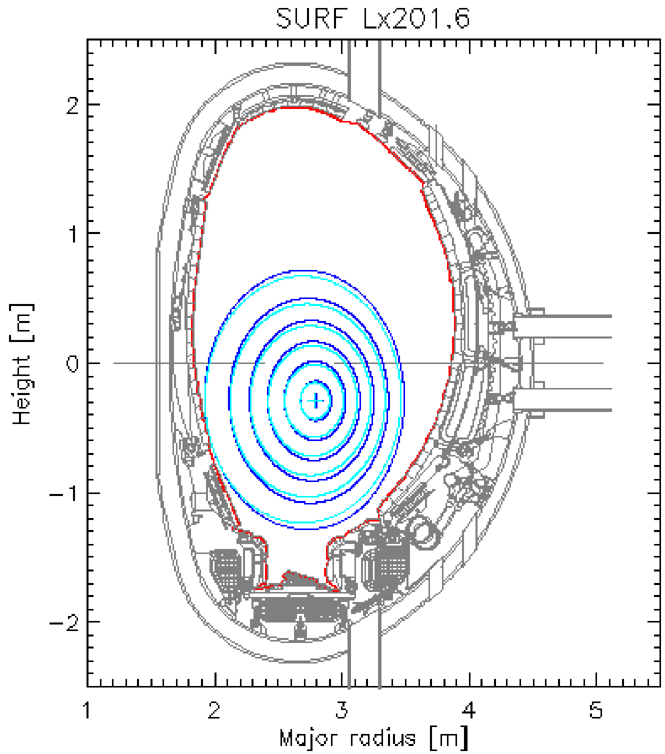

Uncertainties in percentage of counts

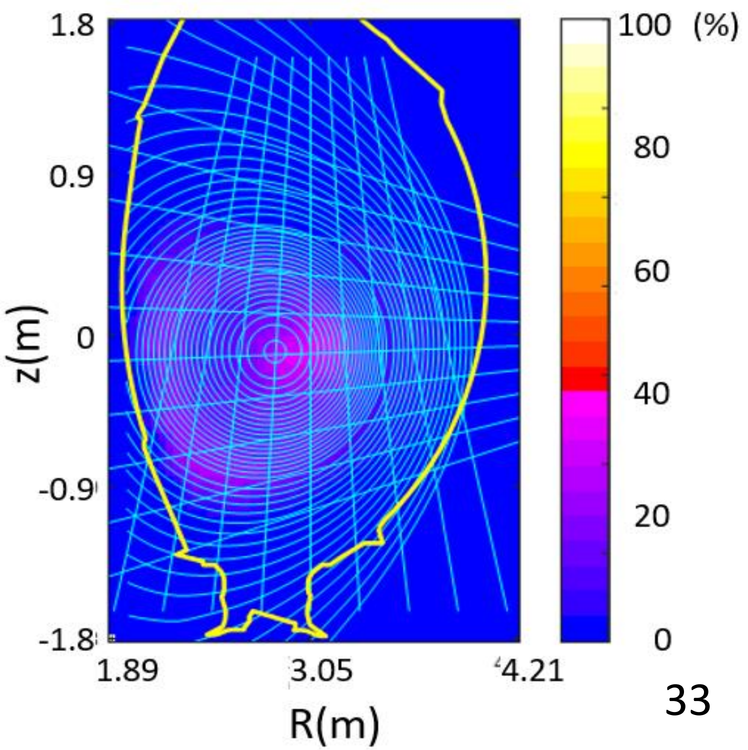

Outline

- Disruptions in the context of control and countermeasures
- Requirements of diagnostics with particular attention to physics and prediction
  - Hardware: Coils, cameras and bolometry
  - Profile indicators
  - Tomography
- Data analysis tools for prediction
- Conclusions and future work

Traditional Predictors

Physics models based on first principles are not available for disruption prediction.

Data driven, machine learning based predictors have been widely studied in the last decades (three installed in JET real time network: APODIS, SPAD, Centroid).

On the other hand the vast majority of predictors are based on traditional forms of learning:

- closed world learning
- separation of feature selection and predictor structures

Closed-World Learning

Traditional supervised Machine Learning is based on the *closed-world assumption:*

- The systems under study must be stationary. The i.i.d. assumption (data independent and identically distributed) means that the results are valid only if the pdf of the data are the same for the training set, the test set and the final application.
- All the classes in the test and final applications must have been seen in the training (with suitable number of examples).

  - **Excessive amounts of data for the training**
  - **Fast obsolescence**
  - **Lack of transferability**

Open-World Machine Learning

Adaptive learning: predictors are updated when appropriate to track the evolution of the phenomena to be predicted. Two main types of adaptation have been implemented for JET to reflect the different time scales involved during and between discharges.

a) Updates of the training sets (including de-learning) and decision functions between discharges

b) Trajectory learning during discharges.

Transfer learning: non supervised clustering to identify new classes (we also transferred one predictor from AUG to JET)

Stacking of Predictors and Classifiers on JET

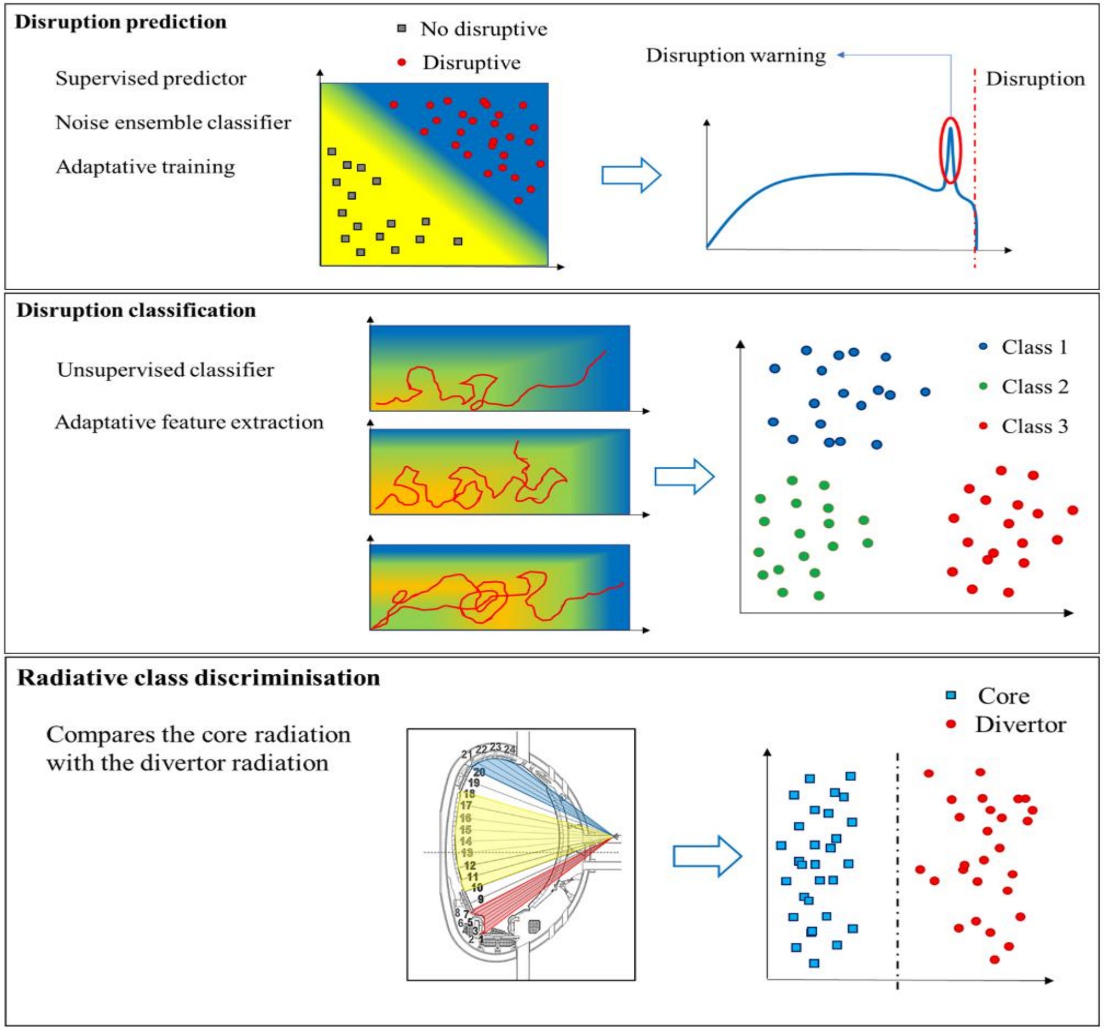

Three layers:

- Predict a disruption is about to occur (Ensembles of CART classifiers)
- Classify the disruption type (K-means)
- If radiative disruption determine whether it is in the core or at the edge.

Implementation from scratch: the predictors operate in real time condition after seeing only one example of disruption

Results for prediction

	Good	Missed	Early	Tardy	All D	False ND	False Alarms	All ND
Counts	576	10	1	0	587	47	48	3014
Percentage	98.13%	1.70%	0.17%	0.00%		1.56%	1.59%	

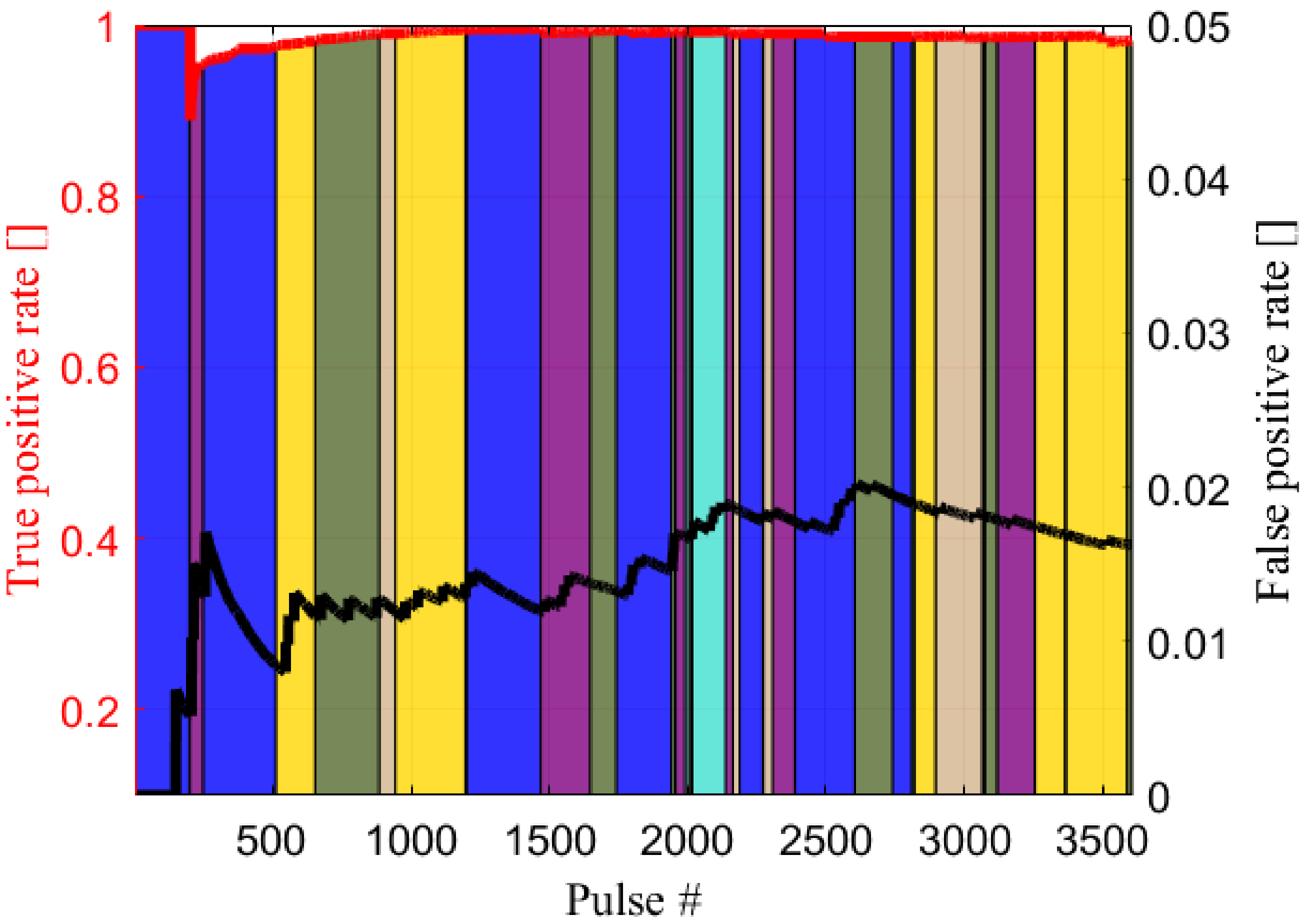

Success rate always above 90% and false alarms never much above 2%.

Statistics conservative.

Results for Classification (K-means)

A disruption is attributed to the class of the first Instability Factor crossing the stability threshold.

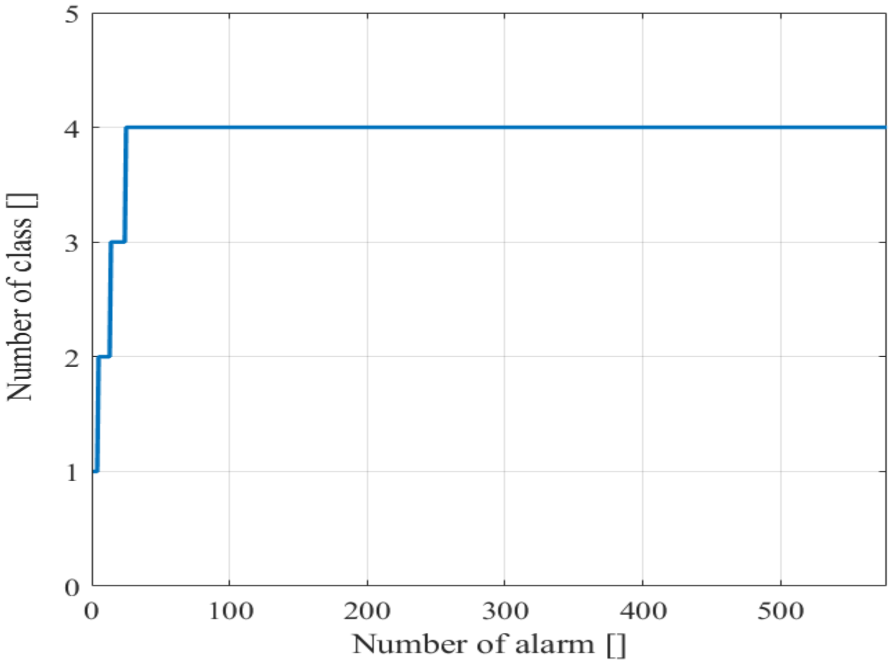

The unsupervised classifier converges rapidly to the four classes expected (in about 40 discharges).

The cumulative plot of the types of disruption

Good agreement with the expert classification

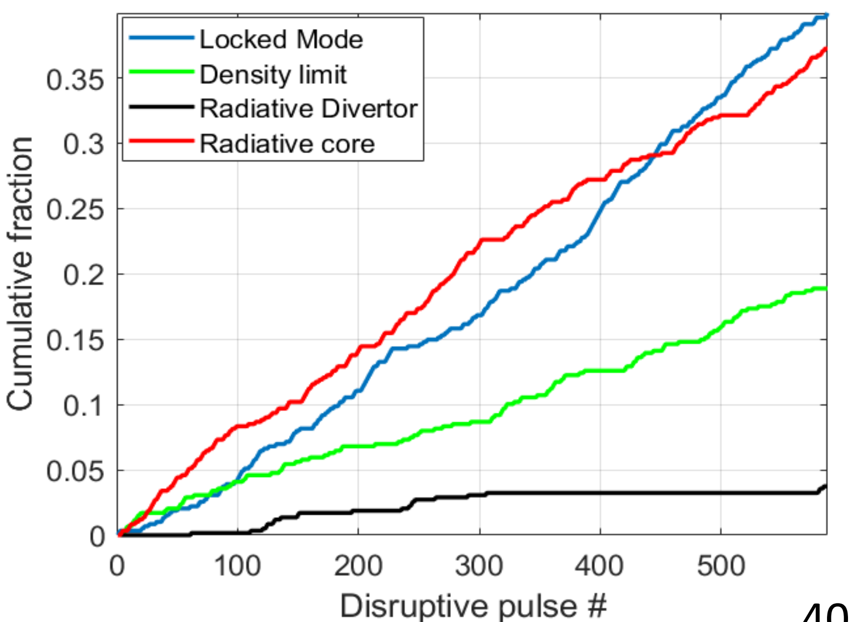

General training scheme with genetic programming

TRAINING/VALIDATION DATABASE

Indicators

Plasma signals (processed and not).

SVM internal params

Which combination is the best one?

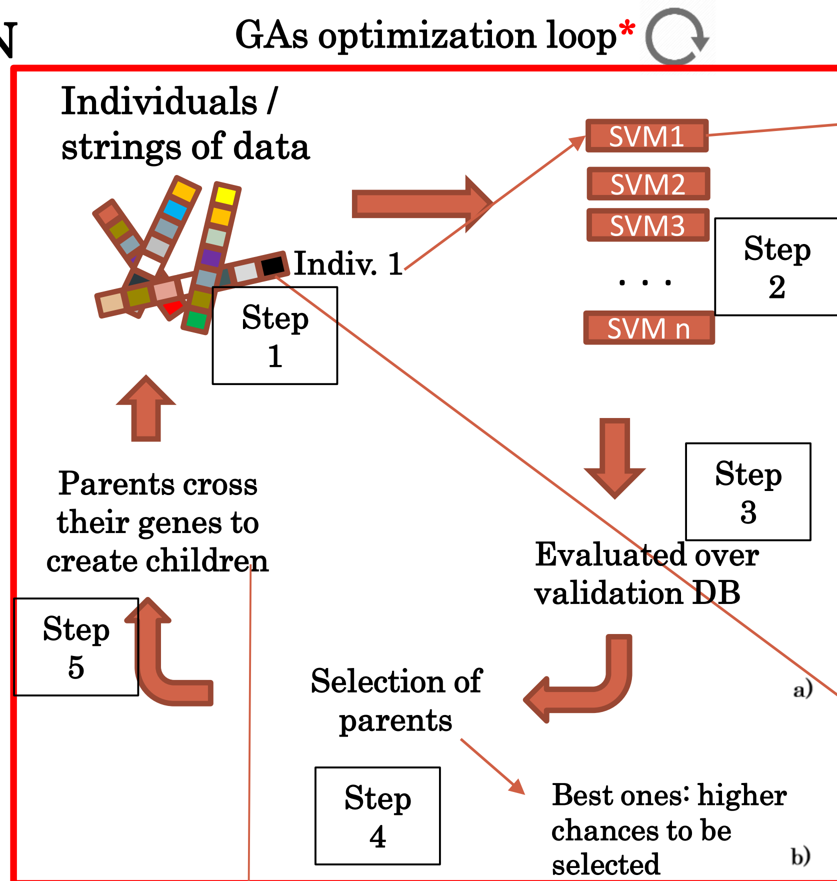

With the instructions written in the strings, the models are trained.

SAMPLES

Samples	Profile (avoidance)	MARFE (prevention)	MIT
Pre-disruptive	20 clear hollow Te/peaked ne from 20 shots	12 shots**	50
Non-disruptive	100	100	200

Ending condition: reach 100 generations

-Population 50 Inds.
-12 hours per run in an Intel(R) Core (TM) i7-8700 CPU @3.2GHz with 16 GB of RAM memory

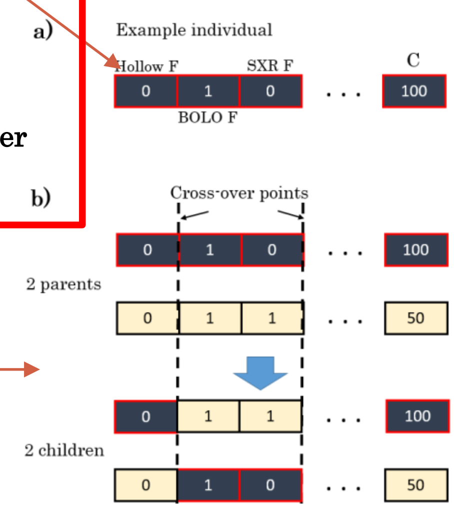

**The phenomenon may remain active along several time-slices in a shot.

*Rattá, G. A., et al. "Global optimization driven by genetic algorithms for disruption predictors based on APODIS architecture." Fusion engineering and design 112: 1014-1018. 2016.

Three detectors for various phases

Total: 974 JET shots (263 of them disruptive and 711 non-disruptive).

Campaign C38 (June 3 – December 20 2019)

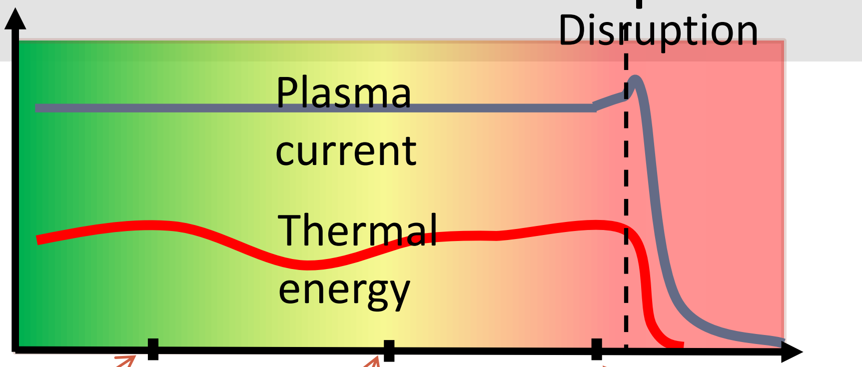

Evaluation every ms from the beginning of the flat top till the end/750 kA of the discharge (also with all the signals available)

PROFILE PREDICTOR

Hollow Te
Hollow ne
Hollow ne_2
Hollow ne_{50}
SXR Factor
SXR $Factor_2$
SXR $Factor_{50}$
BOLO $Factor_2$

MARFEs

ROI 1
ROI 2

RESULTS simulating real-time operational conditions

Detection/ Mitigation

Plasma current
Plasma $current_2$
Total radiated $power_2$
Total Input Power
Total Input $Power_2$
Total Input $Power_{50}$
Mode Lock $amplitude_2$
Plasma Vert. centroid Pos
Plasma Vert. centroid Pos_2

Statistics and warning times

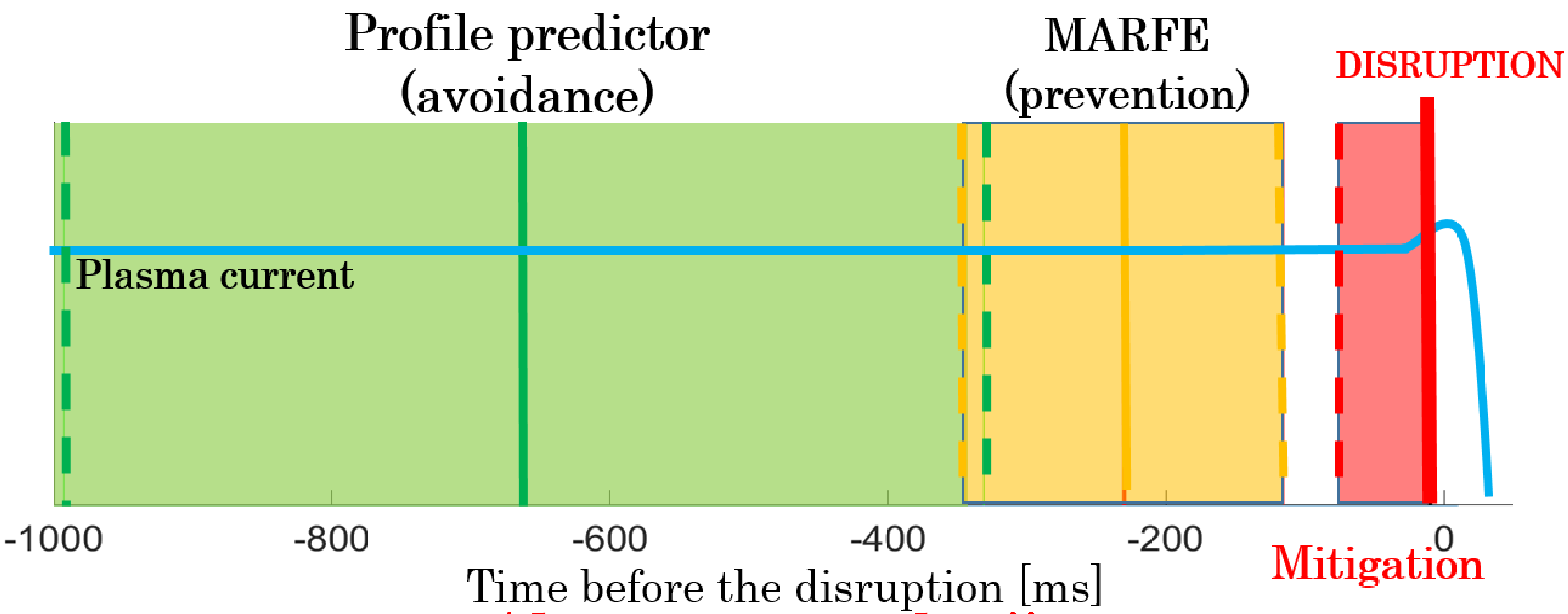

Almost no overlap!!

To each alarm one can associate a minimum time to the disruption and a basic classification of the type

Summary of the results	False alarms 4,7%*	Missed (tardy) alarms 2,3%	Overall success rate 97,7%
Revised stats	1,17%	2,30%	97.70%

Conclusions

- Disruptions remain a major issue for the development of a Tokamak reactor

- The need to understand, avoid, prevent and mitigate disruptions poses significantly specific requirements on various diagnostic systems, which involve:
  - Hardware
  - First signal processing
  - Inversion algorithms
  - Analysis tools for understanding and prediction

- Diagnostic reliability remains of the main problems for real time prediction. Very often the failures have a frequency of more than 10% of the shots whereas the errors of the predictors are in the per cent range.

- The environment of the next generation of devices must be taken into account (accessibility, radiation hardness etc.)

Thanks for Your Attention!

QUESTIONS?

Thermal loads

Main issues: thermal loads depend on the power deposited, the surface and the time (evaporation, melting etc). The surface temperature of the wall materials is difficult to extrapolate because 3D phenomena, broadening of the SOL, heat pulse concentration, convection/radiation ratio etc

Diagnostics:

- Thermography with cameras
- Fast spectrometry for impurity density and temperature.
- Bolometry

Mechanical loads

Main issues: 2D problem of solving self-consistently the plasma movement has been addressed but the extrapolation to ITER is problematic.
The 3D problem of determining the toroidal asymmetries of the forces is not solved and can be very delicate.

Diagnostics:

- Coils in different toroidal locations (at least 4) for resolved equilibrium reconstructions
- Measurements for toroidal vessel currents and halo currents also at different toroidal locations and poloidally resolved.
- Accelerometers, strain gauges, displacement measurements on the vessel and supporting structures.

Seeding Experiments: Krypton

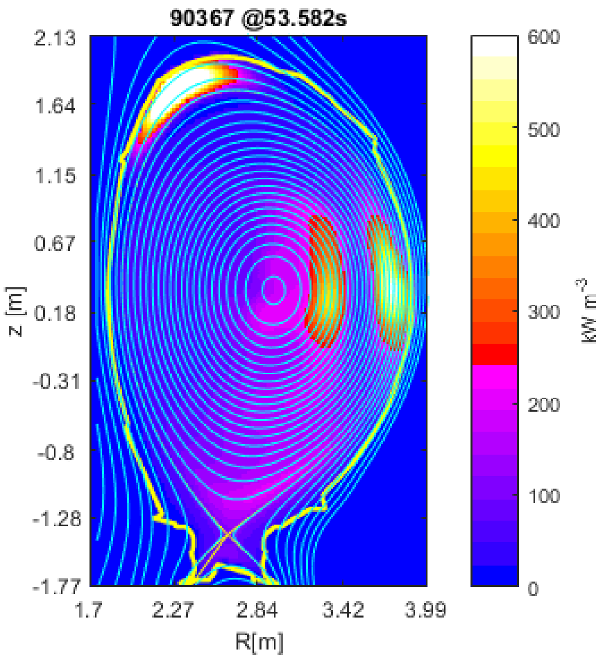

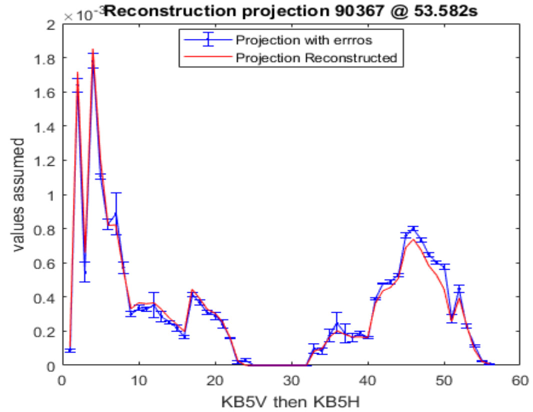

In discharges with Kr the phenomenology is different. No sign of formation of a MARFE type of high radiative zone above the X point.

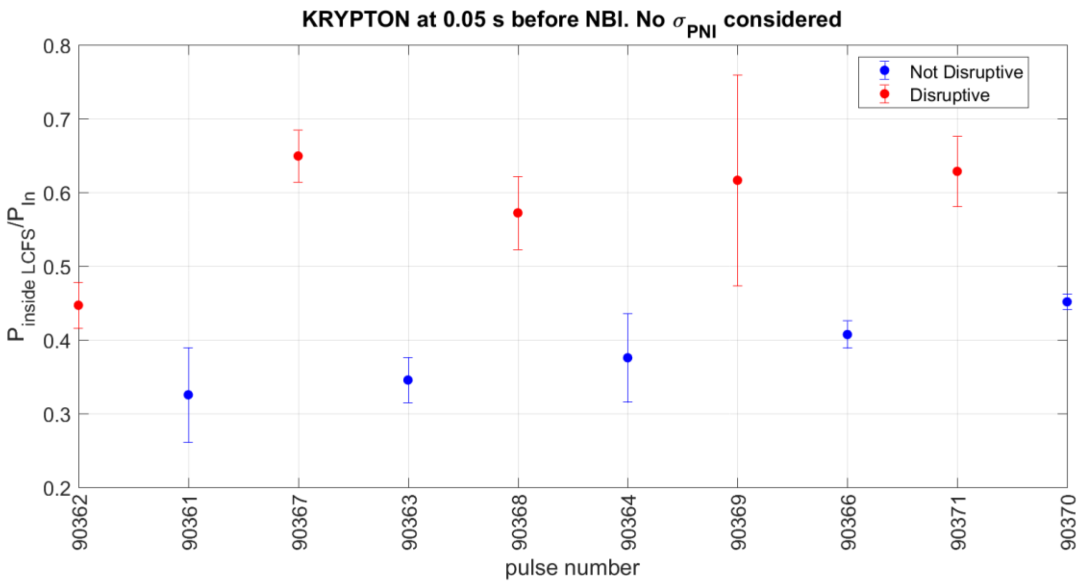

Max radiated fraction achieved is 65%

The radiation seems to be due to a threshold in the radiation inside the LCMS

Low spatial resolution tomography

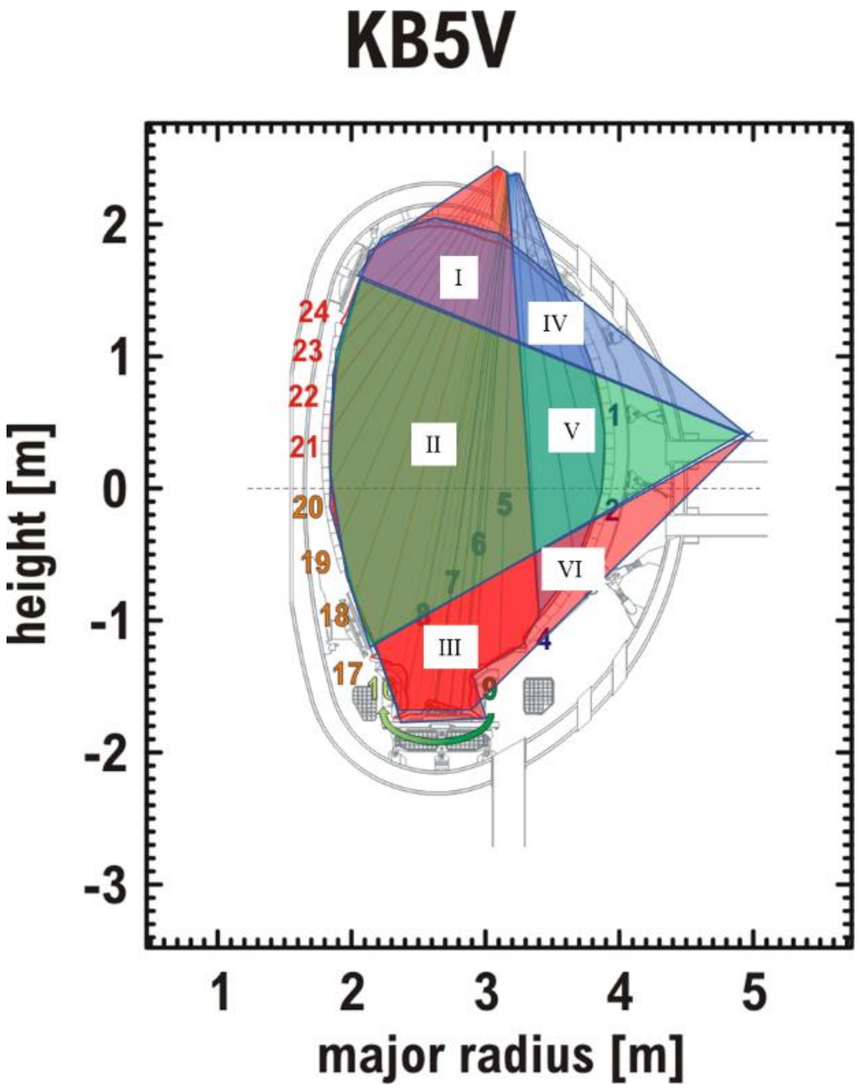

$$H_1 = R_{III}$$

$$H_2 = R_{II} + R_V$$

$$H_3 = R_I$$

$$V_1 = R_V$$

$$V_2 = R_I + R_{II} + R_{III}$$

Under the assumption that the emission in regions IV and VI is negligible, the system can be solved.

Effects of neutrons on materials

- **External irradiation station**
  - An External Irradiation Station has been designed and installed to locate samples as close as possible to the plasma edge to maximise the fluence
  - Two sample holders (RADA + ACT) and optical fibres
  - Method of removing samples after DTE2 has been developed and tested
  - **ACT:** 26 samples, 1-mm thick (or more with reduced thickness) to investigate activation of structural

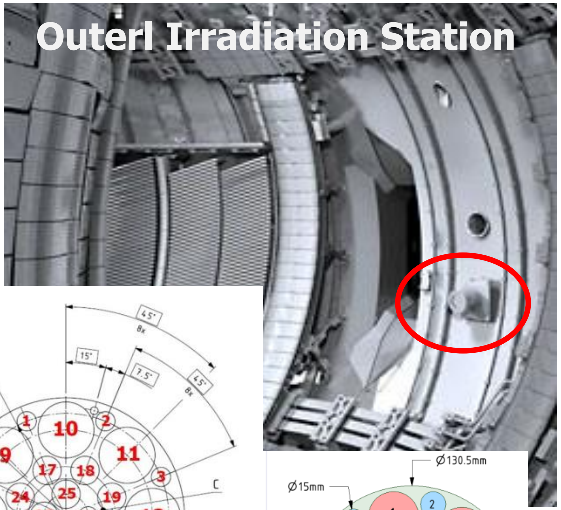

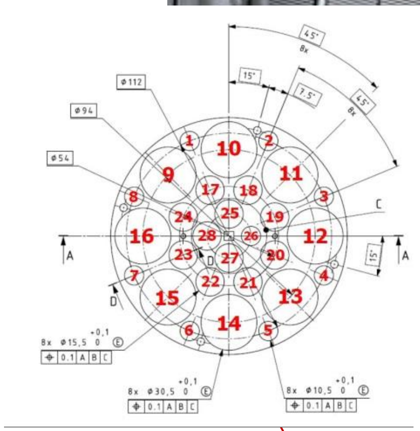

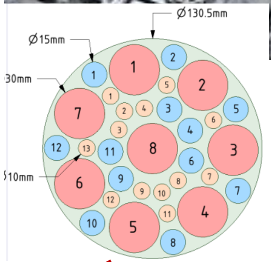

Unexpected Zn-65 and Ta-182 found in steel samples

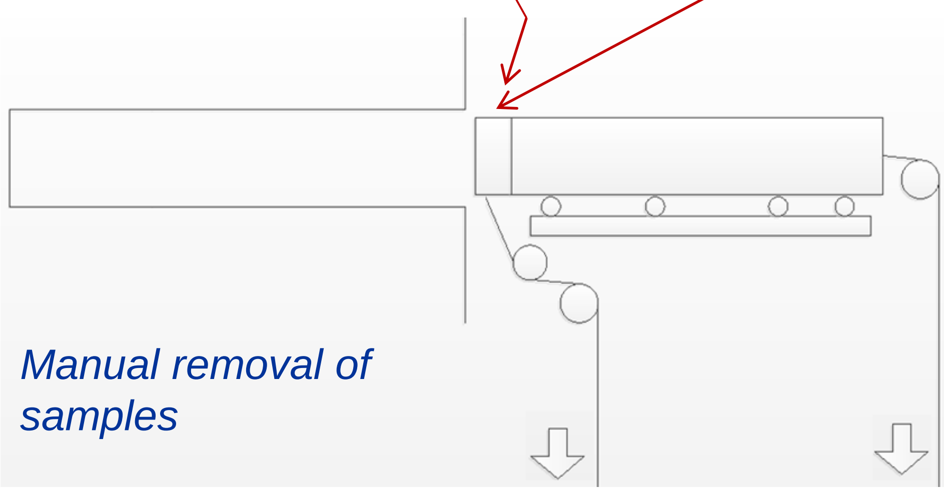

Manual removal of samples

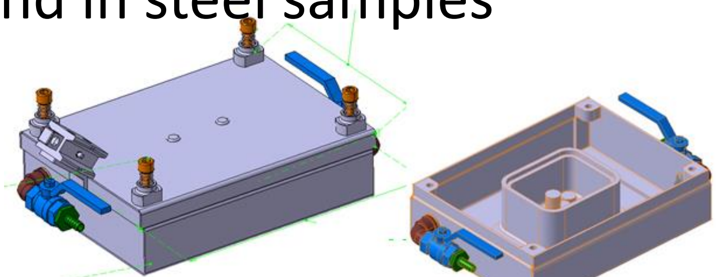

Lead-lined sample case

Radiation damage in functional materials

Measurement of the radiation damage in functional materials due to 14 MeV neutrons. 64 samples

- **Materials selected (Zirconium oxide rejected due to expected high activation)**
- **Particular care paid to finding materials with low impurities**
- **The Aim is:**

1. **Active Optical measurements**
   - Radiation induced optical absorption (RIA) & luminescence (RL) in fibres
2. **PIE Measurements**
   - Electrical conductivity
   - Radiation induced conductivity (RIC)
   - Loss tangent and Permittivity (from kHz to GHz's).
   - Rad. induced absorption (RIA) and
   - Radio-luminescence (RL) (VUV-UV-VIS-IR).

Material	Manufacturer	Coating
SAPPHIRE	several	yes
SAPPHIRE	several	no
Alumina	several	no
F.SILICA	Tydex UV	no
F.SILICA	Tydex IR	no
MgAl2O4	several	yes
MgAl2O4	several	no
BaF2	2	Yes
BaF2	2	No
CaF2	2	yes
CaF2	2	No
YAG	2	No
ZnS	Crystran	Yes
ZnS	Crystran	No
Diamond		No
AlN	Kyocera	No

JET comprehensive disruption mitigation system (DMS)

DMV1	Upper port	4.6m to LCFS
DMV2	Horiz. port	2.8m to LCFS
DMV3	Upper port	2.4m to LCFS

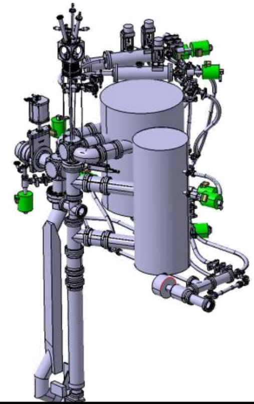

Massive gas injection <u>mandatory</u> in JET for:
- ❑ Ip > 2MA **OR**
- ❑ $W_{TH}+W_{MAG}$ > 5MJ

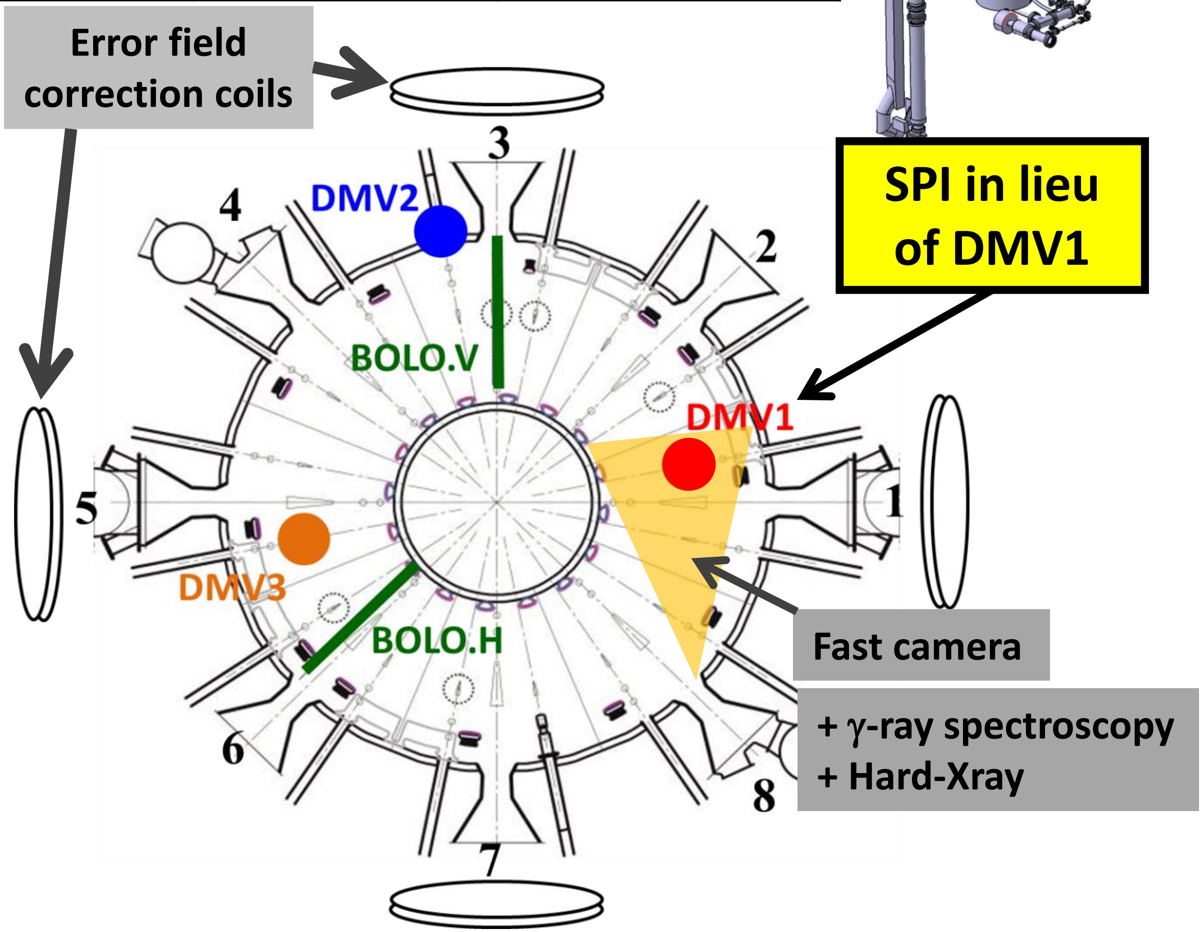

- Massive Gas Injection: conversion to radiation not meeting ITER requirements
- No suppression of runaways electrons
- Shattered pellet in operation